A New Hubble Expansion Probe and Cosmological Constraints

Manolis Plionis

National Observatory of Athens & Univ. of Thessaloniki

Roberto Terlevich , INAOE(Mexico) & IoA University of Cambridge
Elena Terlevich,INAOE
Fabio Bresolin, IfA-Hawaii
Jorge Melnick, ESO
Spyros Basilakos, Science Academy-Athens
Eduardo Telles, Observatorio Nacional, Rio de Janeiro
Ana Luisa Gonzalez, INAOE
David Fernandez Arenas, INAOE
Ricardo Chavez, Cavendish Lab. University of Cambridge
Pavlina Tsiapi, National Capodestrian Univ & Academy of Athens

Corfu, 9-9-2022

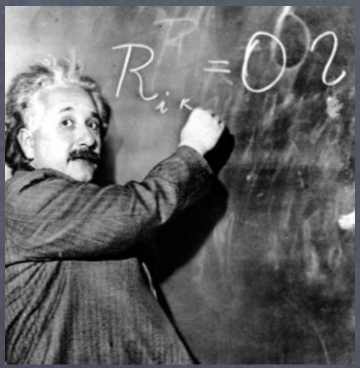

A Mathematical description of our Universe

$$H^2 = \left(\frac{\dot{a}}{a}\right)^2 = \frac{8\pi G\rho}{3} - \frac{kc^2}{a^2} + \frac{\Lambda c^2}{3}$$

Energy Conservation

A useful representation of the source terms is that of virtual fluids with (ρ,P)

$$H^2 = \left(\frac{\dot{a}}{a}\right)^2 = \frac{8\pi G}{3}\left[\rho_m + \rho_k + ...\right]$$

parametrization of ρ_i as fractional contribution to the global energy density

$$\Omega_i(a) = \frac{\rho_i}{\rho_{\text{total}}} = \frac{8\pi G\rho_i}{3H^2}$$

+

$$\rho(a) = \rho(0)\left(\frac{a}{a_0}\right)^{-3(1+w)}$$

$$P = w\rho c^2$$

$$\boxed{\Omega_m + \Omega_k + .. = 1 \quad \forall z}$$

Important relation between Ωs which just reflects mass conservation

The 1st Friedmann eq. can now be written in the form (known as Hubble relation):

$$H^2(z) = H_0^2\left[\Omega_r(1+z)^4 + \Omega_m(1+z)^3 + \Omega_k(1+z)^2 + \Omega_w \exp\left(3\int_0^z \frac{1+w(x)}{1+x}dx\right)\right]$$

The main Cosmological parameters that we seek to determine in order to define the Cosmic Dynamics are: H_0, Ω_m , Ω_k , Ω_w , w(z)

$$w(z) = w_0 + w_1 f(z)$$

$$f(z) = z/(1+z)$$

Hubble expansion Probe (SN Ia)

Type-Ia Supernovae (SNe Ia) result from explosion of White Dwarf having accreted mass from a companion star, beyond the critical Chandrasekhar limit (~ 1.4 M$_\odot$).

In 1998 two teams (Perlmutter, Riess) found that distant SNIa are dimmer than expected, a fact interpreted as being due to an accelerated expansion of the Universe. Ever since the new accumulation of data and better understanding of systematics confirm constantly this interpretation.

$$\mu = m - M = 5\log_{10} D_L + 25 \quad + \quad D_L = (1+z)\int_0^z \frac{c}{H(z)}\mathrm{d}z \quad \longrightarrow \quad \mathbf{H(z)}$$

$$H^2(z) = H_0^2\left[\Omega_r(1+z)^4 + \Omega_m(1+z)^3 + \Omega_k(1+z)^2 + \Omega_w \exp\left(3\int_0^z \frac{1+w(x)}{1+x}dx\right)\right]$$

$$\chi^2(\mathbf{p}) = \sum_{i=1}^{n} \frac{\left[\mu_{\mathrm{th}}(z_i,\mathbf{p}) - \mu_{\mathrm{obs}}(z_i)\right]^2}{\sigma_i^2}$$

χ2 minimization provides
Cosmological parameter space

Hubble expansion Probe (SN Ia)

A COMPREHENSIVE MEASUREMENT OF H_0 FROM SH0ES 31

Riess et al. 2022

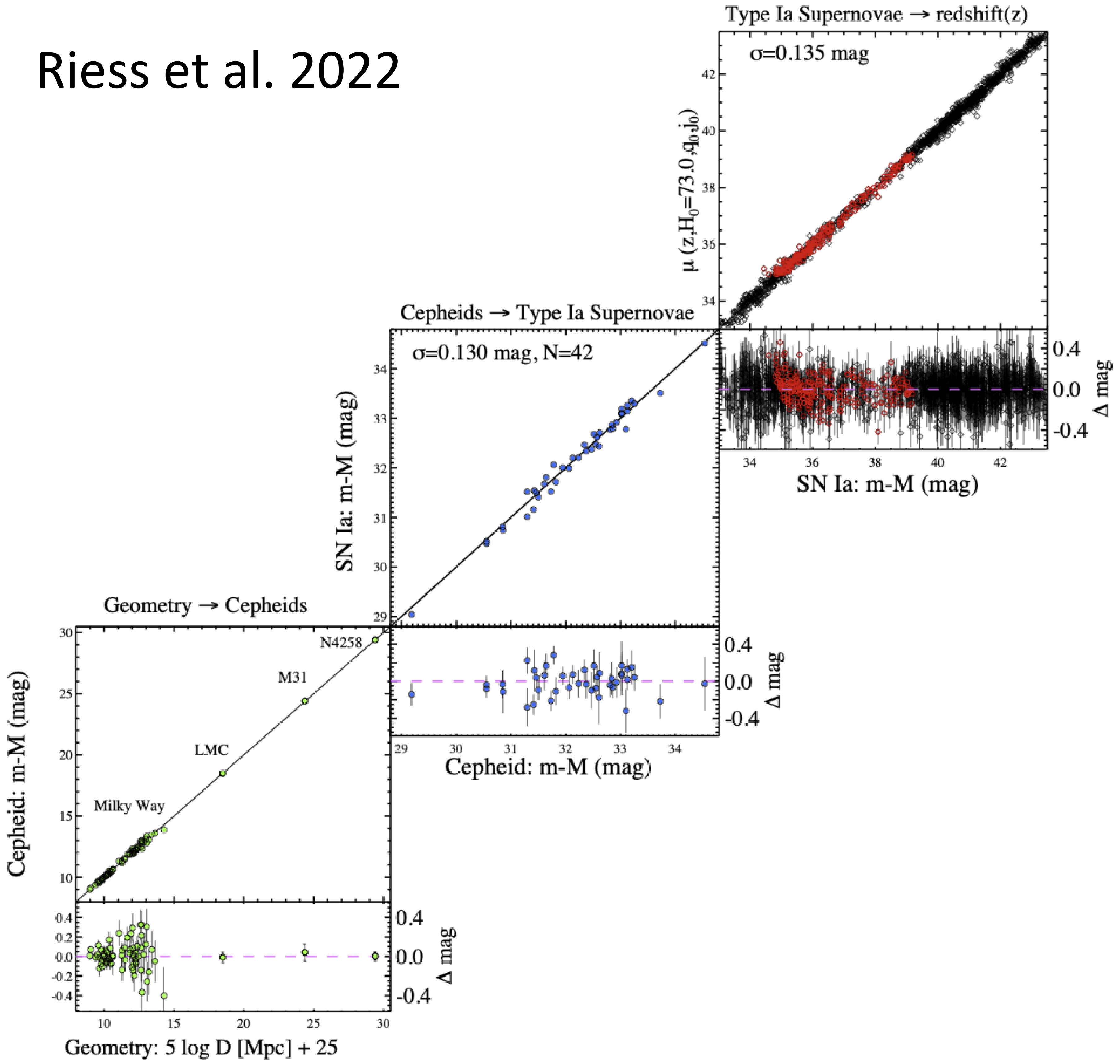

Which are the optimum depths in order to differentiate between different DE models?

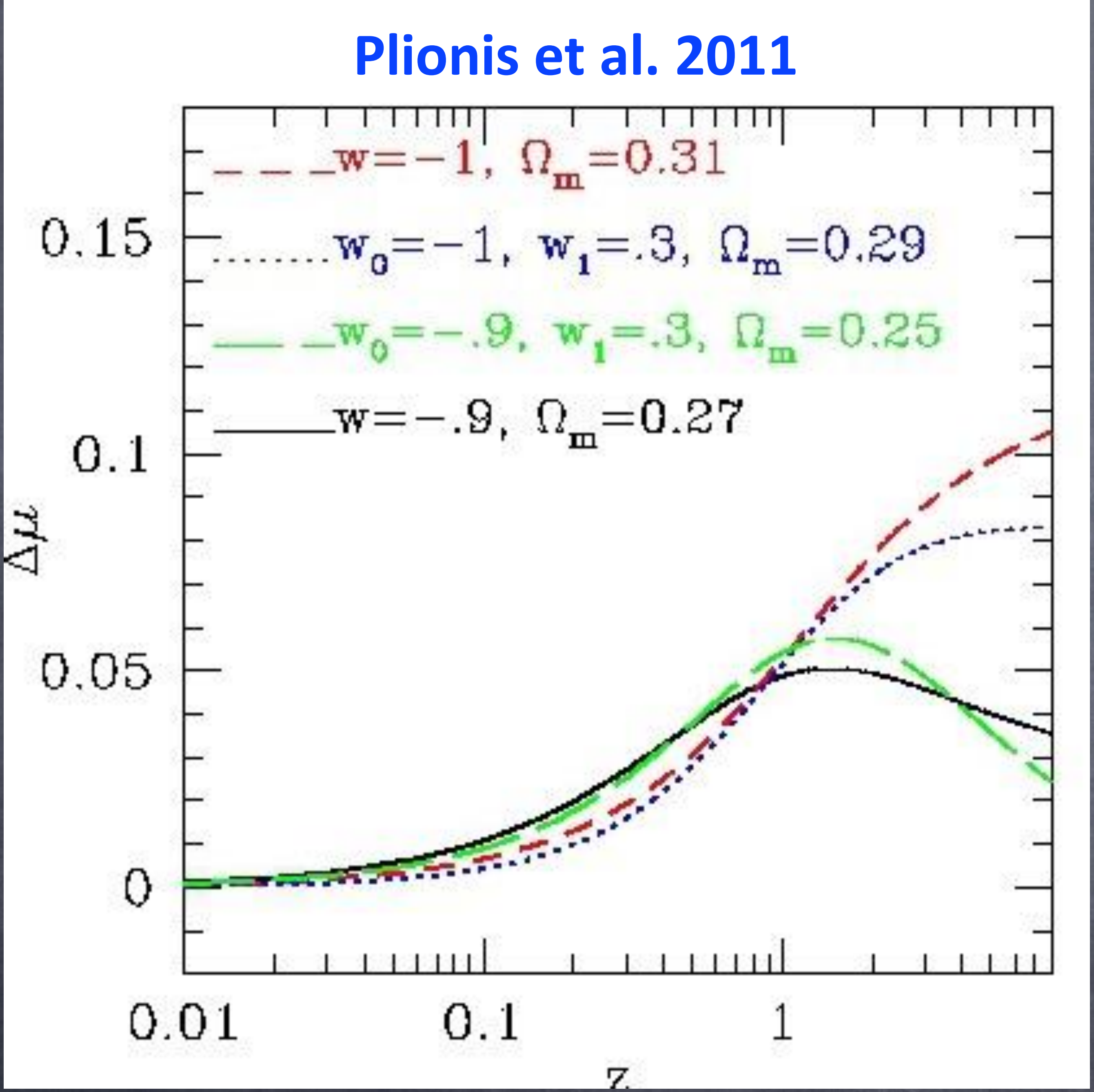

Important observation: the largest differences between models occur at **z>2**

Conclusion: It would be ideal to have tracers of the Hubble expansion that go deeper than z=2

Severe Problem: Degeneracies of Cosmological parameters

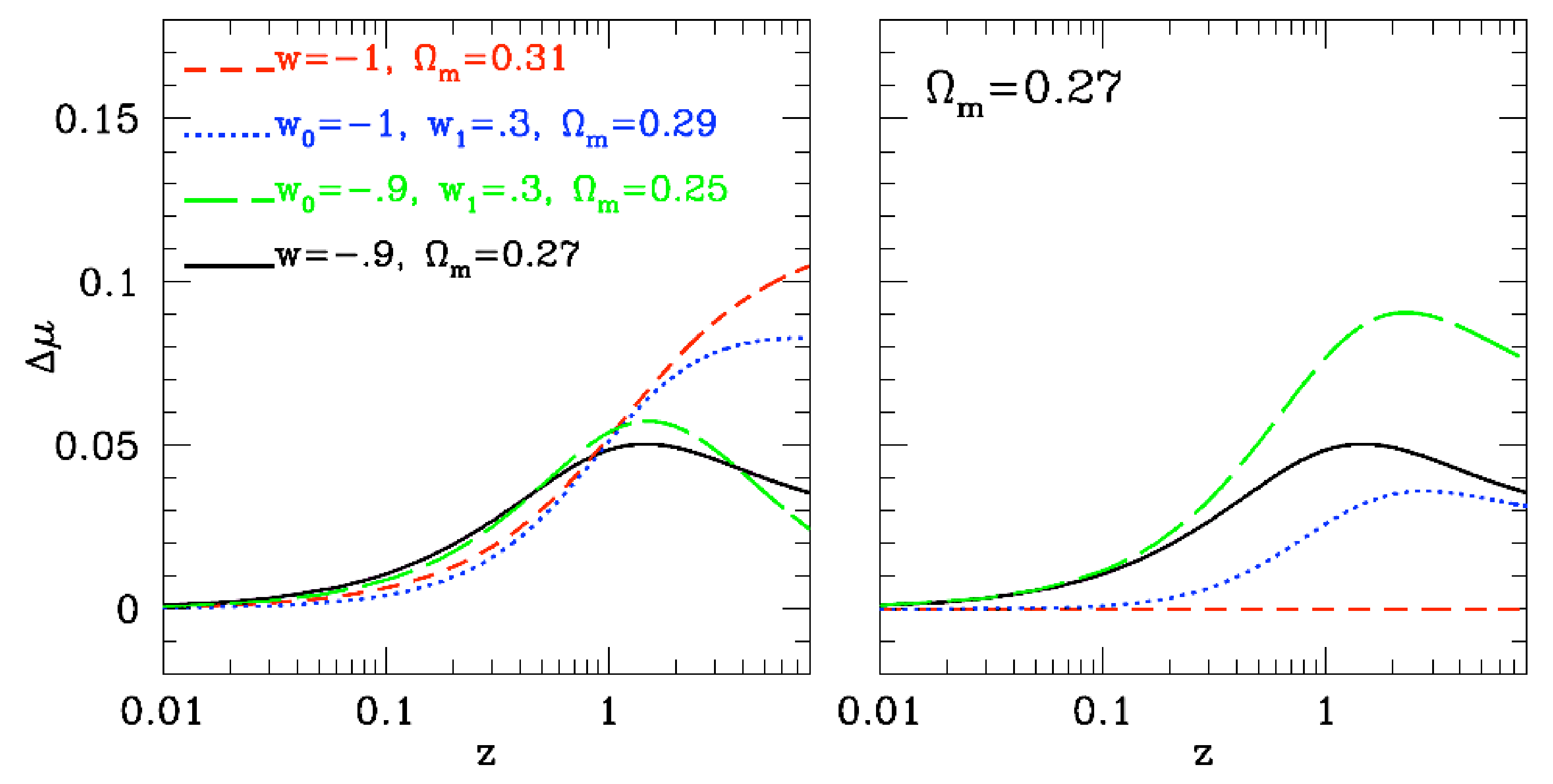

Important observations:

(1) the largest differences between models occur at $z>1.5$-2, and

(2) Necessary to break degeneracies (eg., estimating independently Ω_m)

To break degeneracies it is necessary to join different Cosmological Probes in order to get useful constraints on parameters:

Degenerate Solutions to Observations

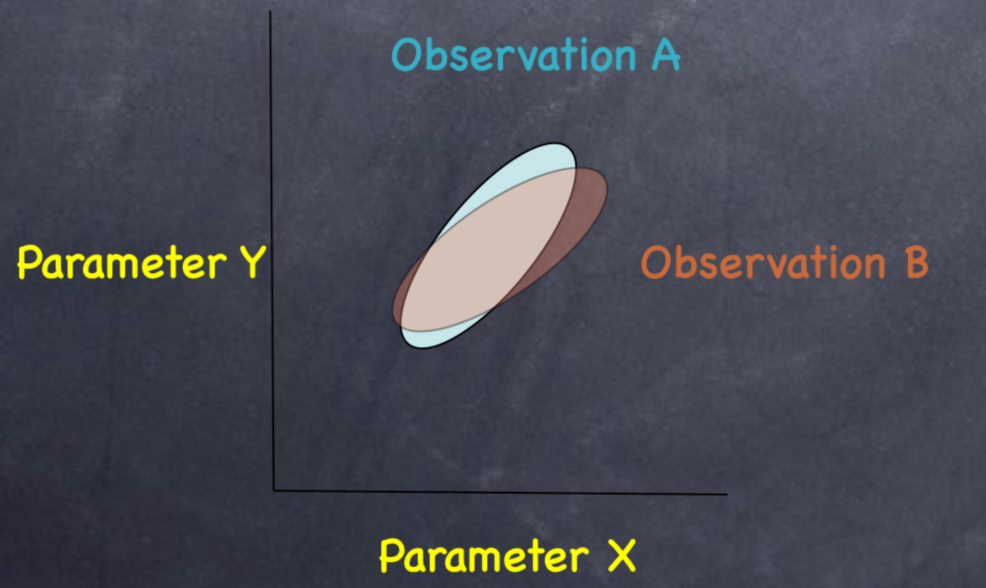

Non-Degenerate Solutions to Observations

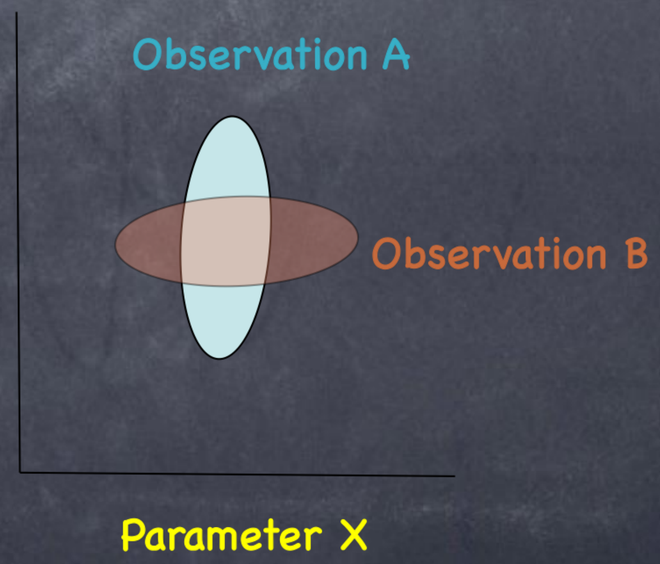

High-z probes & effect of Grav.Lensing

Extensive Monte-Carlo Simulations to test methodology

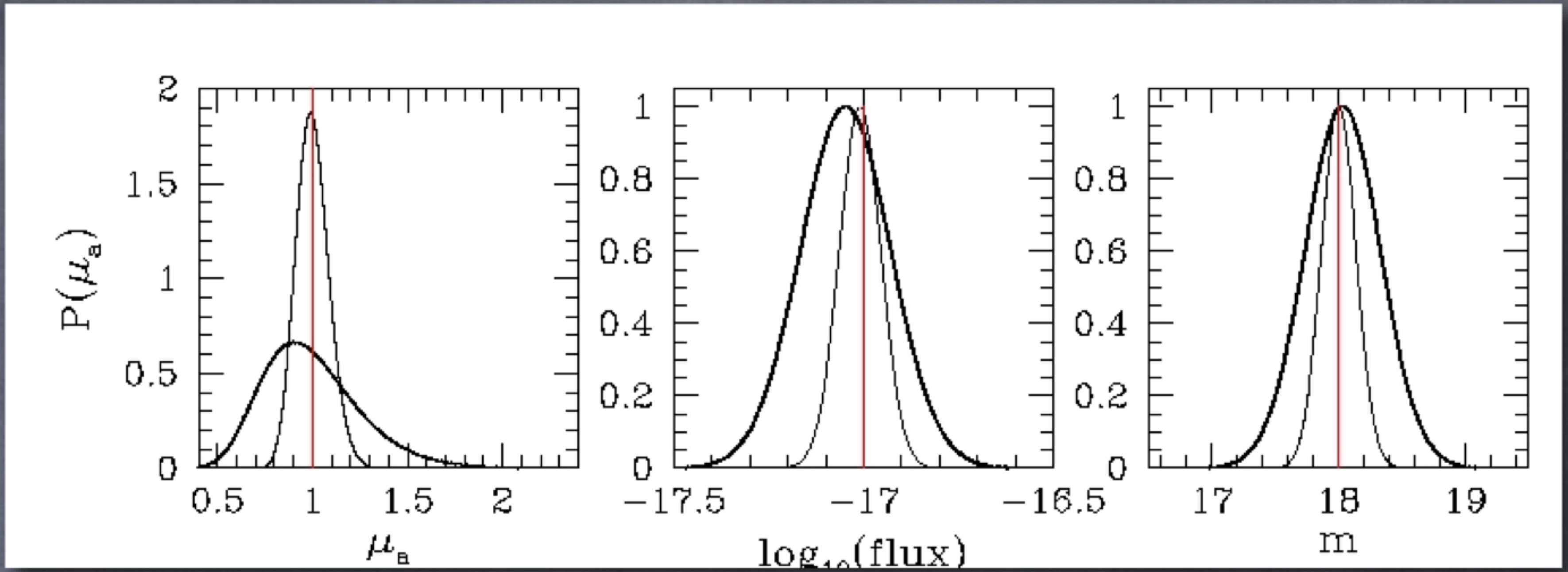

Plionis et al. 2011

(eg., Holz & Wald 1998; Holz & Linder 2005; Brouzakis & Tetradis 2008). Assuming a Robertson-Walker background superimposing a locally inhomogeneous universe and taking into account both strong and weak lensing effects, results in a magnification distribution of a single source over different paths which is non-Gaussian. The magnification probability density function $P(\mu_\alpha)$ resembles a log-normal distribution with $\mu=0$ (mean flux over all possible different paths is conserved since photon numbers are unaffected by lensing), with the mode shifted towards the de-magnified regime with a long tail to high magnification.

Thus most sources will be de-magnified, inducing an apparently enhanced accelerated expansion, wh few will be highly magnified.

A NEW H(z) TRACER

GRECO-LATIN Collaboration

INAOE, Aristotle Univ., Academy of Athens, Obs. of Hawai, ESO
(collaborators: Terlevich, R., Terlevich, E., Plionis, M., Basilakos, S., Bressolin, F., Melnick J., Telles, E., Chavez, R.)

Two basic necessities make the use of a new H(z) tracer an important task:

(a) Consistency check of the Cosmological results based only on one class of high-z tracer (SNIa).

(b) The need to go much deeper in redshift in order to break degeneracies between different DE models.

A NEW H(z) TRACE

Our approach is to use HII galaxies (**compact galaxies with massive burst of SF, generated by the formation of SSC's, found in dwarf irregulars and dominating total L)** and their local counterparts **Giant HII regions**. Optical spectra dominated by strong Balmer lines, produced by gas ionized by the massive SSC. The Higher the Star cluster mass, larger the No of ionizing γ, larger the motions of the gas) —> Tight correlation between L(H$_\beta$) and stellar velocity dispersion, **σ** (Melnick & Terlevich 1981; Melnick et al. 1988; 2000).

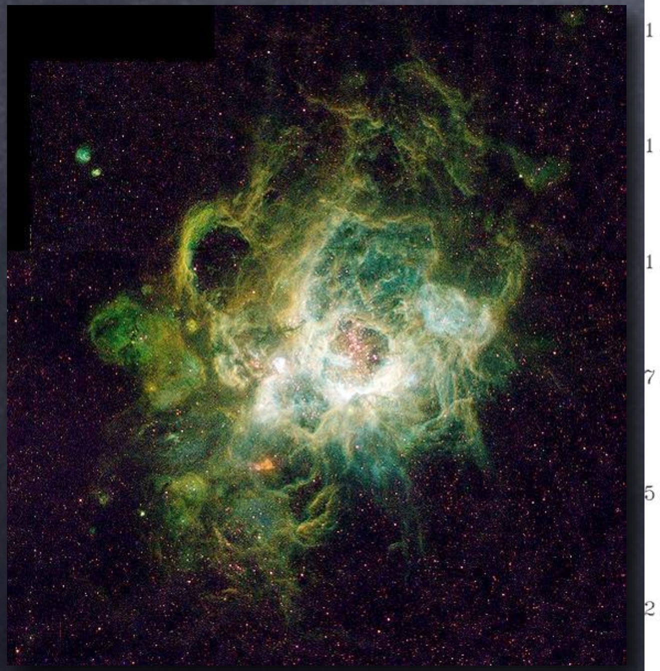

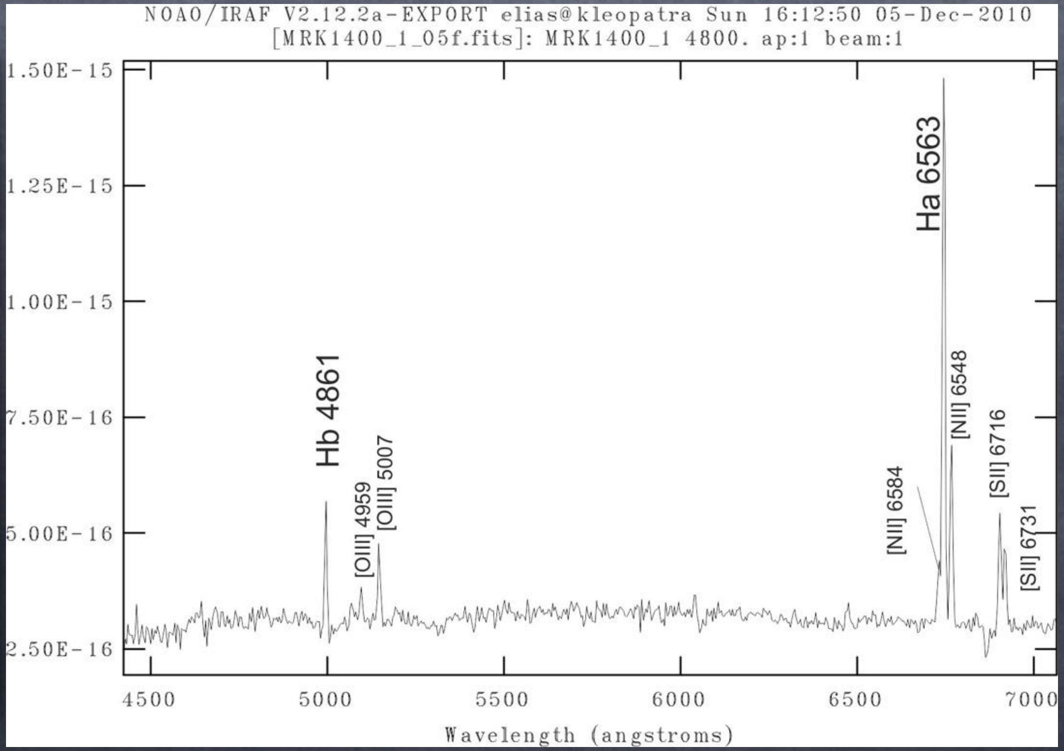

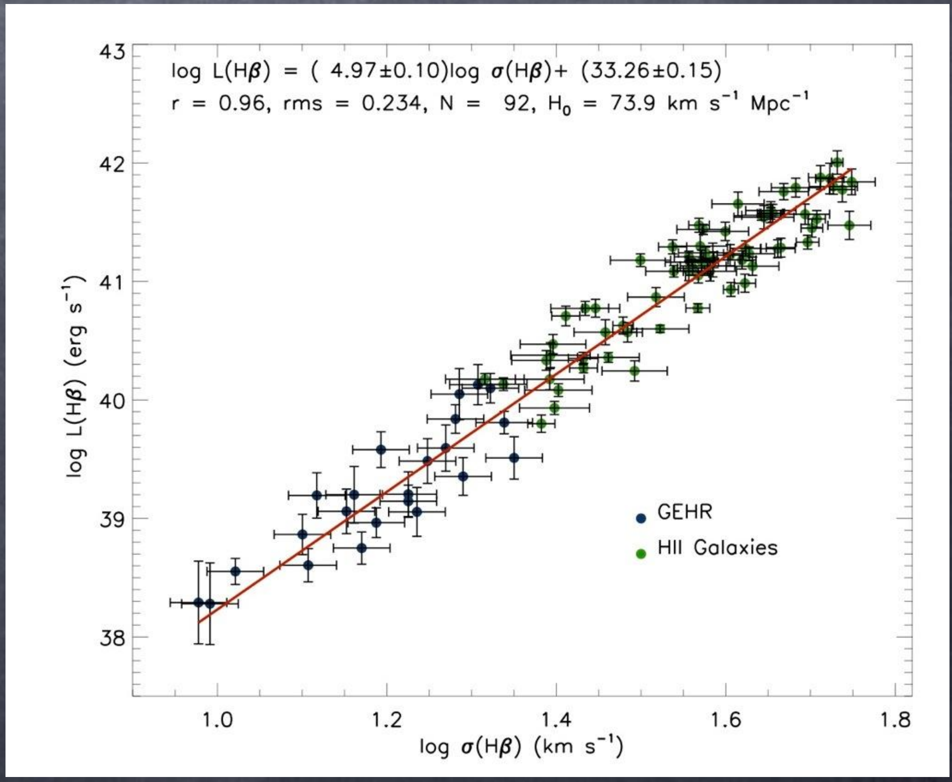

HII Galaxies = The youngest and most massive SSC

1. Selected from spec-surveys by strong narrow emission lines with **EW(Hβ) > 50Å or EW(Hα) > 200Å in order to have an upper age-limit (~ 5Myr), and limited contamination by an older stellar population.**

2. **compact size to reduce inter-cluster dynamics.**

Thus luminosity of HII galaxies is almost completely dominated by the young burst

they are larger versions of the giant HII regions found in outer regions of late spirals

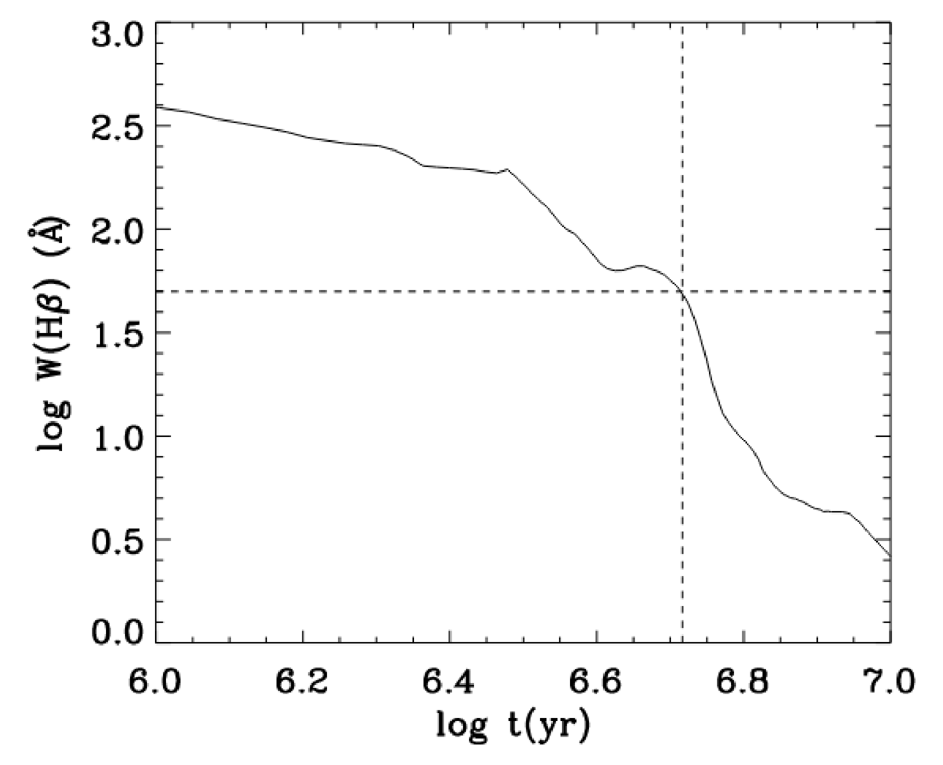

From SB99+Salpeter IMF for instantaneous burst

The observed properties of HIIG and GHIIR are those of a very young Super Stellar Cluster (SSC) with almost no parent-galaxy contamination

Giant HII regions

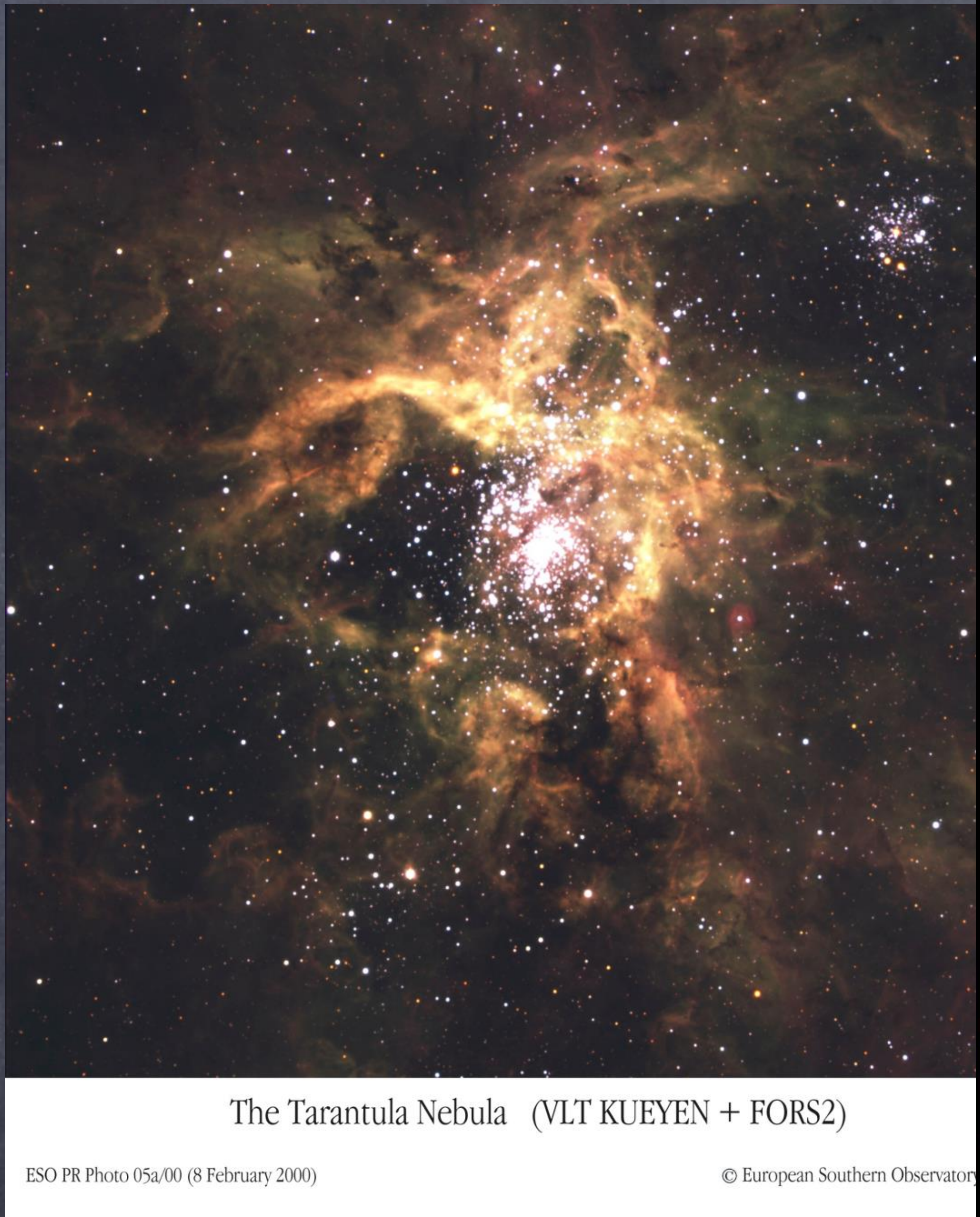

The Tarantula Nebula (VLT KUEYEN + FORS2)

ESO PR Photo 05a/00 (8 February 2000)

© European Southern Observatory

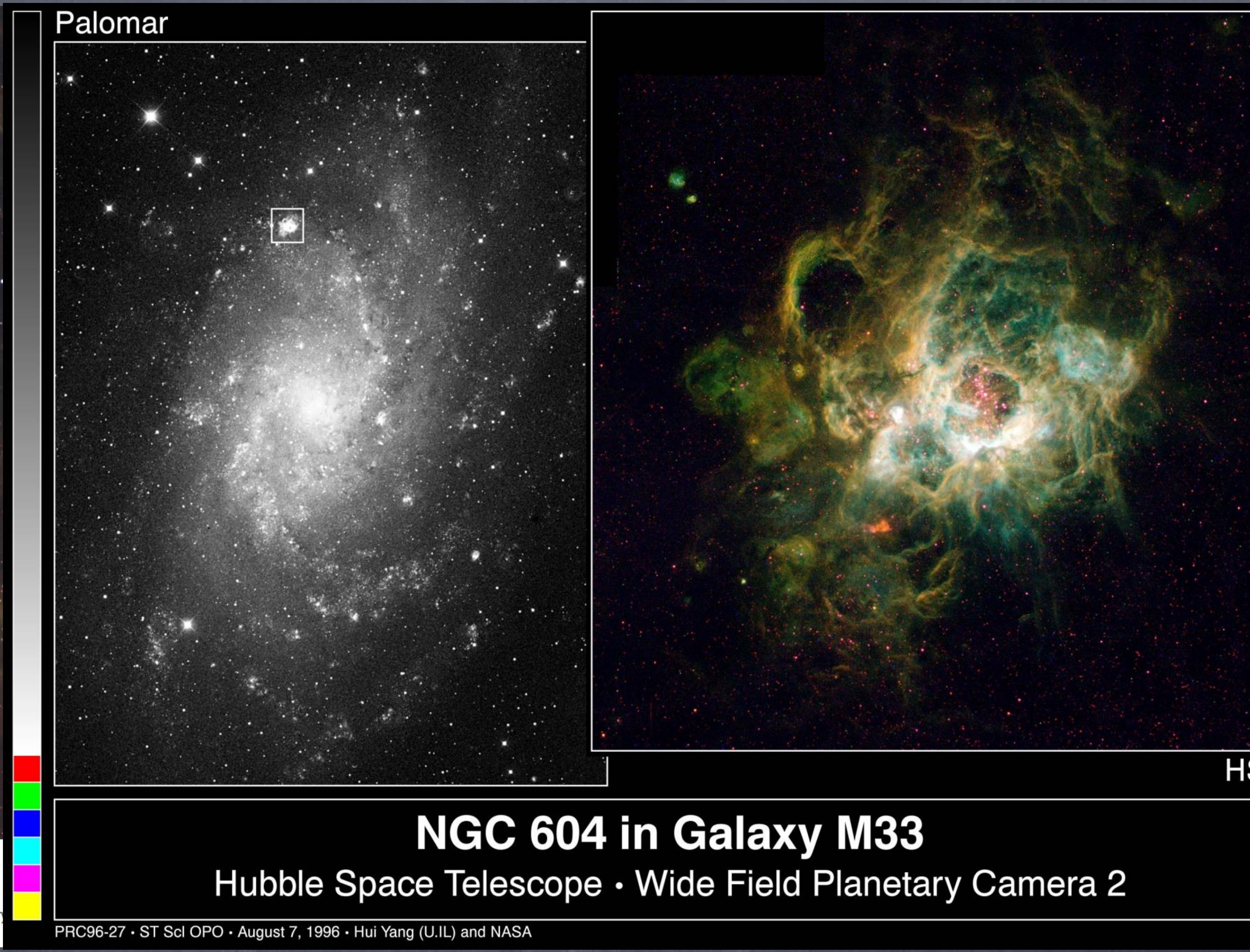

NGC 604 in Galaxy M33

Hubble Space Telescope • Wide Field Planetary Camera 2

PRC96-27 • ST ScI OPO • August 7, 1996 • Hui Yang (U.IL) and NASA

30 Doradus: Prototype

HII Galaxies: Low-z sample

We select 128 HII galaxies from the spectroscopic DR7 SDSS catalogue within $0.01<z<0.16$
Their characteristics are: compact, with large Hβ fluxes and equivalent widths (EW). The clean sample after excluding peculiar line profiles, double lines, or rotationally broaden lines is 92 HII galaxies.

Telescopes used:

Subaru 8m, VLT 8m, Keck 10m

SPM & Cananea 2.1m (integrated fluxes)

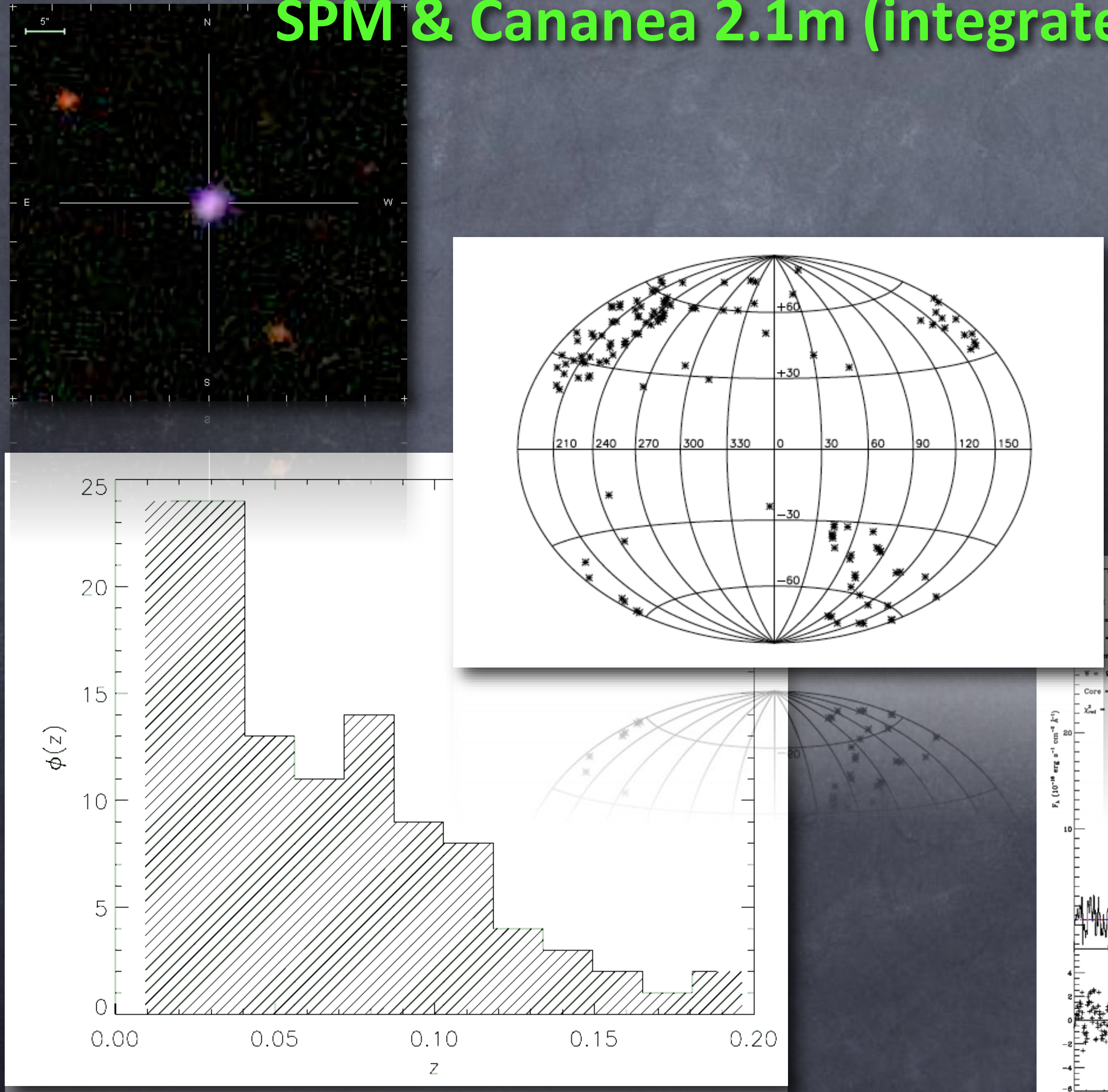

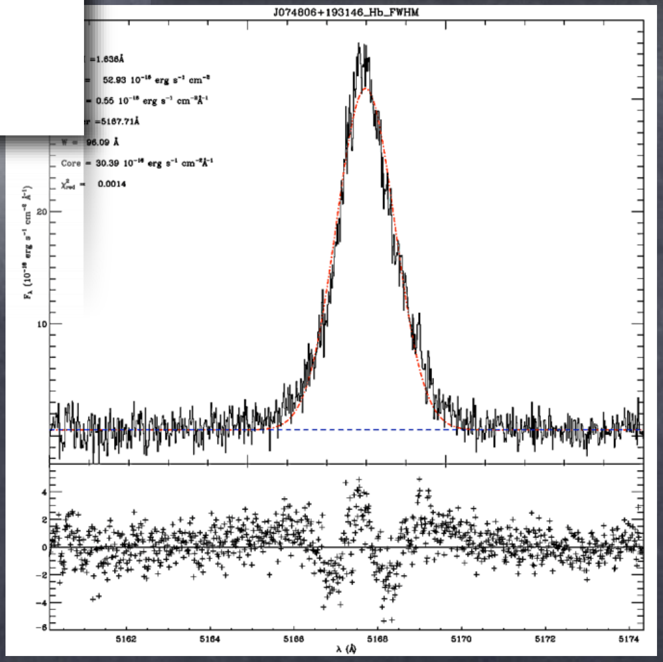

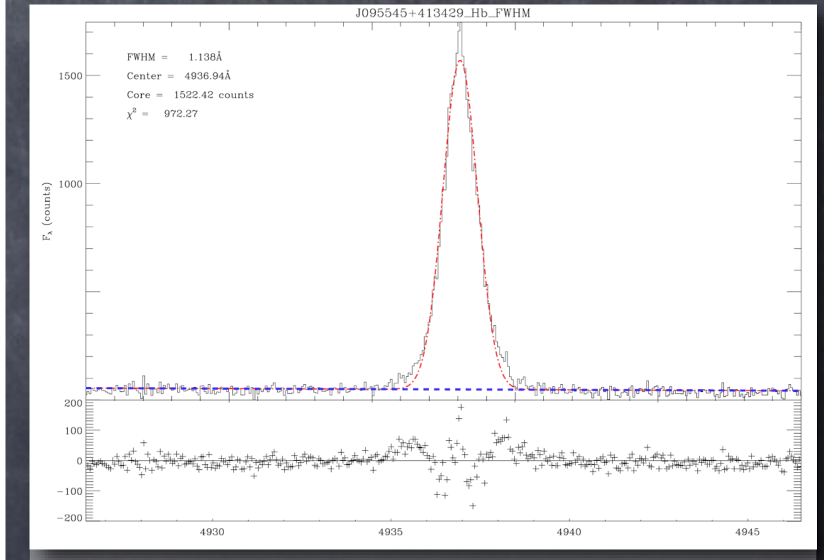

SDSS Stamp Images of H II Galaxies

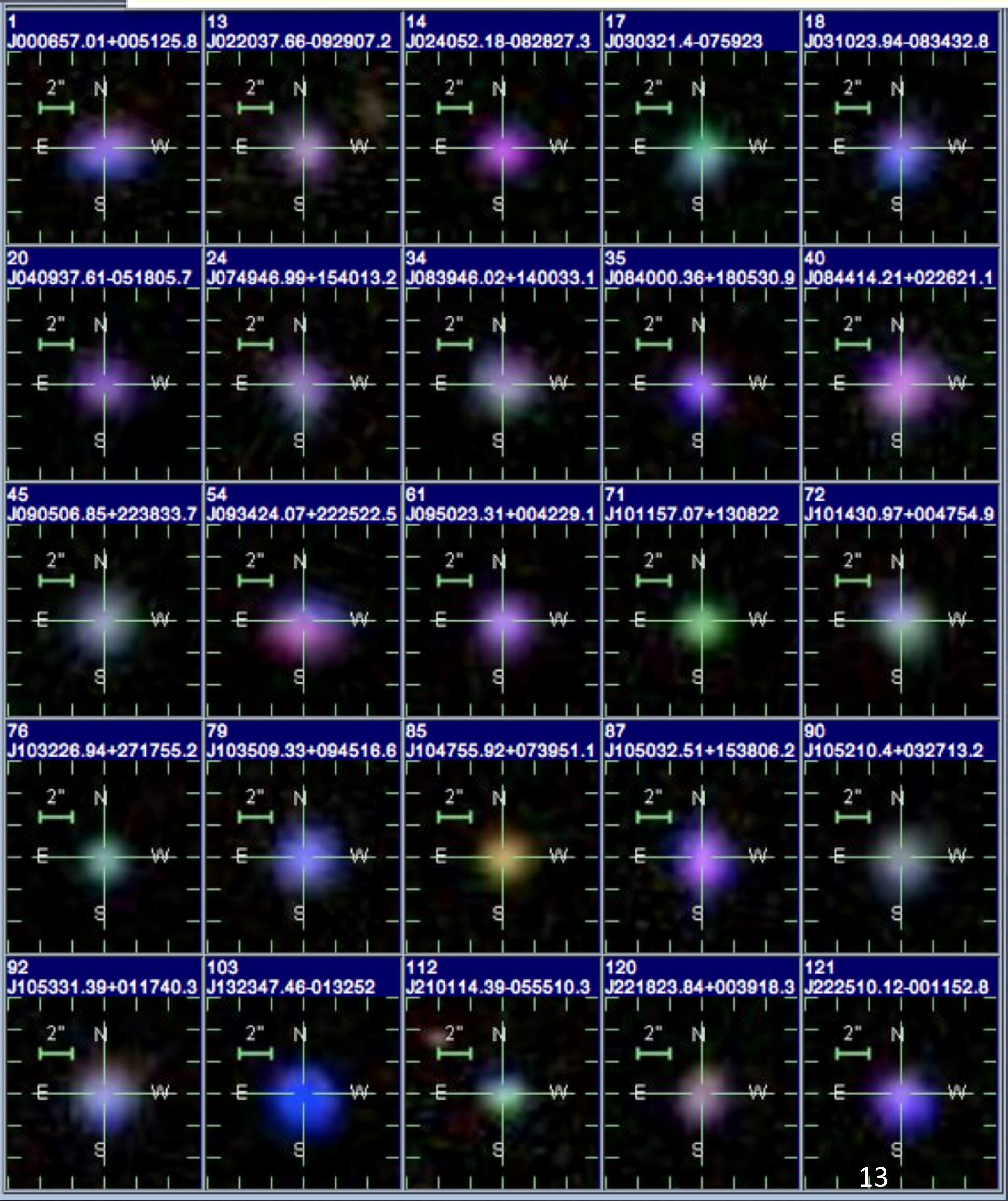

The sample of HIIG was selected from SDSS as having:

$0.01 < z < 0.20$
EW(Hβ) > 50Å
R_{Petro} < 3 arcsec

The colour in these SDSS stamp images depends on redshift.

Some are green most are not.

The L-sigma relation for HIIG and GHIIR

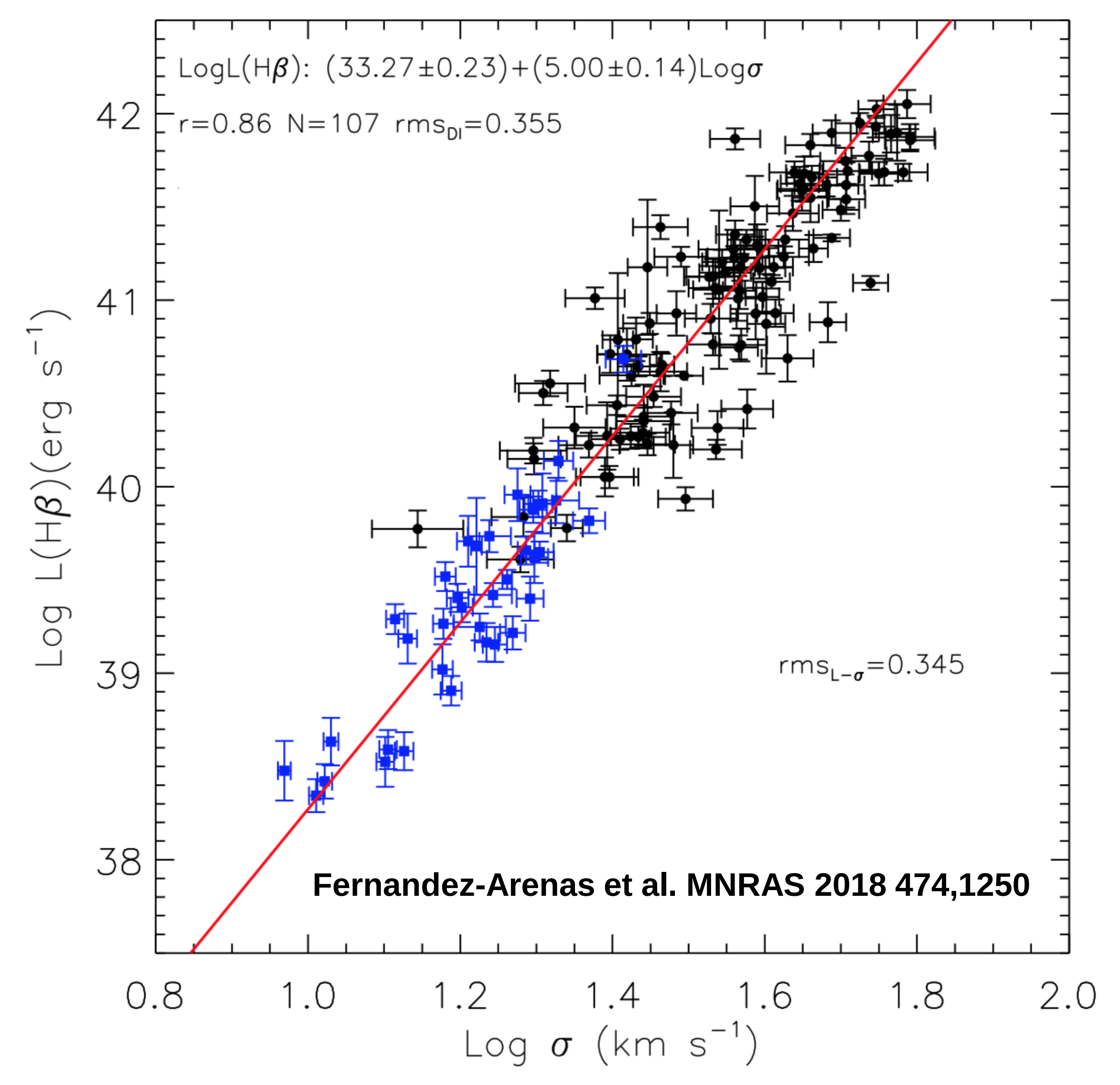

Fernandez-Arenas et al. MNRAS 2018 474,1250

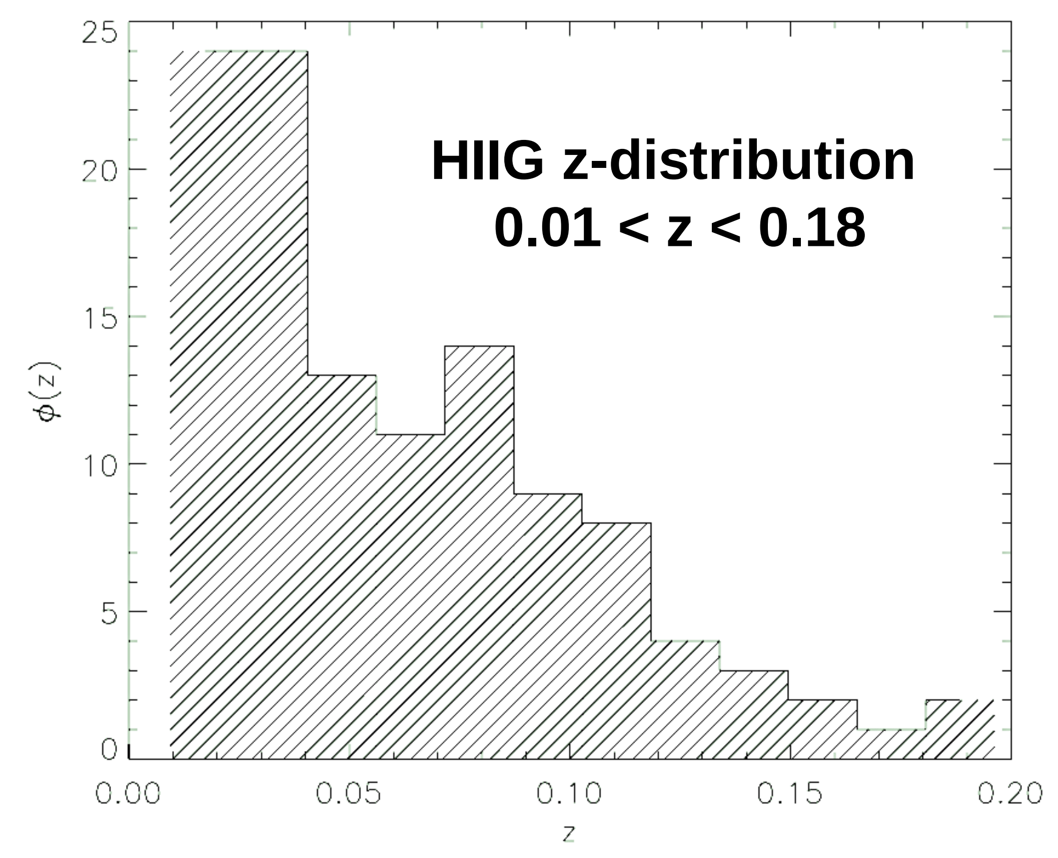

HIIG z-distribution
0.01 < z < 0.18

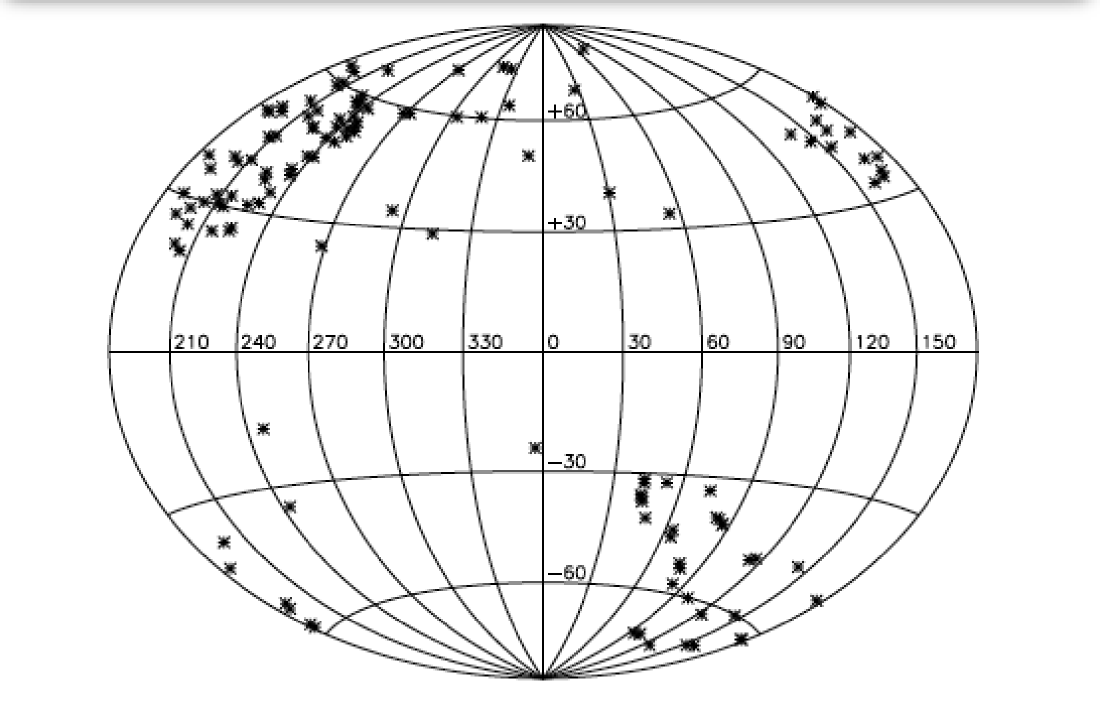

107 HII galaxies and 36 giant HIIR in 13 galaxies with Cepheids distances.

1st Application: Low-z HII H_0 estimation

Methodology to Estimate Ho

- Determine the slope of the L(Hβ)-σ distance indicator, using the HII galaxy sample.

- Determine the intercept of the relation (the zero-point) using the local calibration `anchor' Giant HII region sample + Cepheid & TRGB distances.

- Use a χ2 minimization procedure to find which value of Ho minimizes the difference between the HII galaxy luminosities predicted from the derived L(Hβ)-σ relation, and those estimated from the Hβ flux and the distance based on a grid of Ho values.

$$\chi^2(H_0) = \sum_{i=1}^{n} \frac{[L_i(\sigma_i, a, b) - \tilde{L}_i(H_0, f_i, z_i)]^2}{\sigma^2_{L,i} + \sigma^2_{\tilde{L},i}}$$

1st Application: Low-z HII H_0 estimation

Measuring H_0

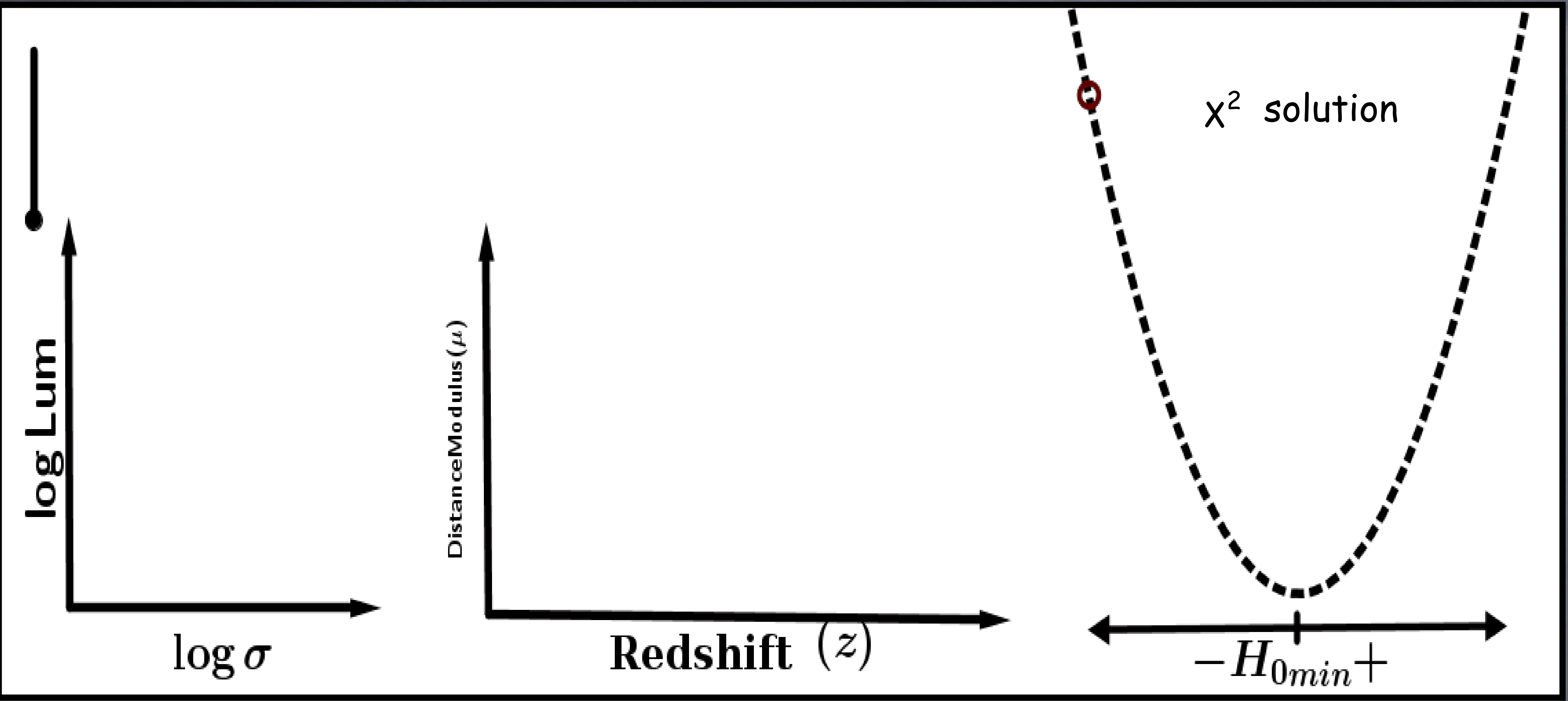

L - sigma - Size relation and the viral theorem

The phenomenological L-σ relation supported by viral theorem. A weak dependence on size also indicates that the L-sigma relation is a 2-D projection of a 3-D fundamental plane, L-sigma-size.

$M_{Dyn} = \eta\ G^{-1}\ R_{Eff}\ \sigma^2$ (coefficient η depends on density profile).

Assuming **M/L=Constant** we get $L = \eta\ G^{-1}\ R_{Eff}\ \sigma^2$ or $\underline{L \propto R_{Eff}\ \sigma^2}$

From fit: $\underline{L \propto R^{1.05}\ \sigma^{2.52}}$

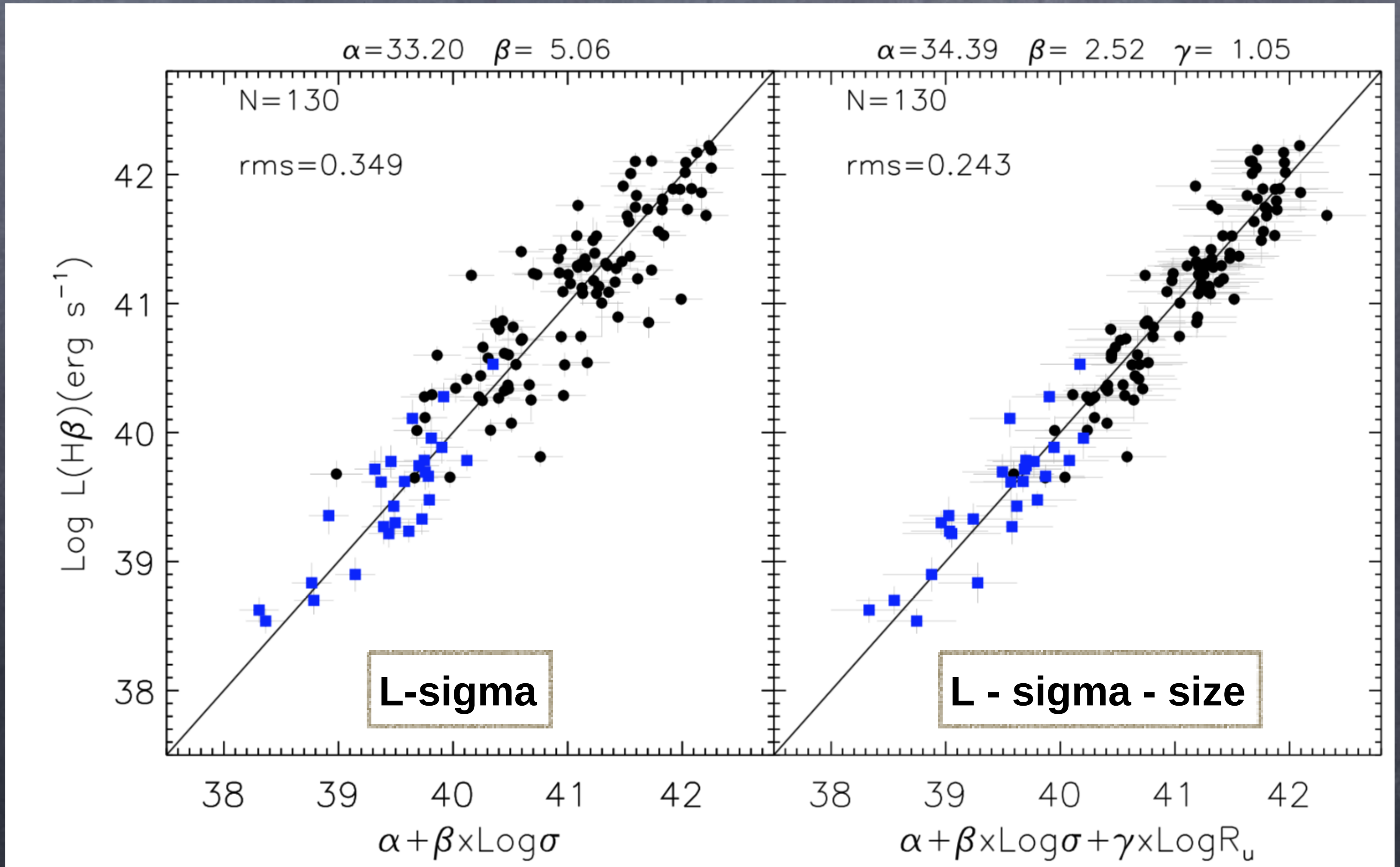

The Fundamental Plane of HIIG and GHIIR

The three projections of the fundamental plane

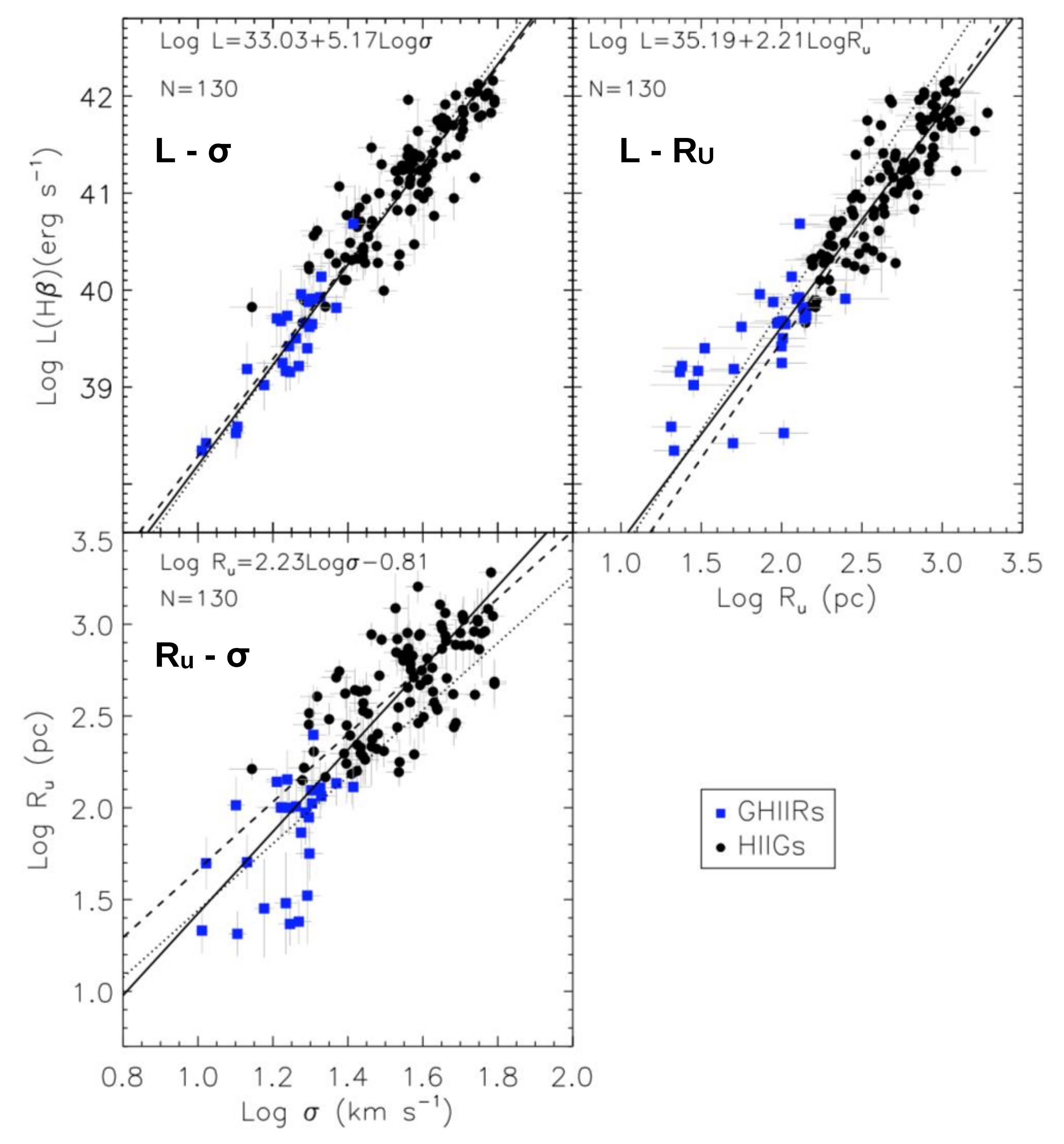

H0 determination - GHIIR Anchor Sample

The anchor sample consist of 36 GHIIR in 13 galaxies with accurate determination of distances via Cepheids.

Fernandez Arenas et al 2018

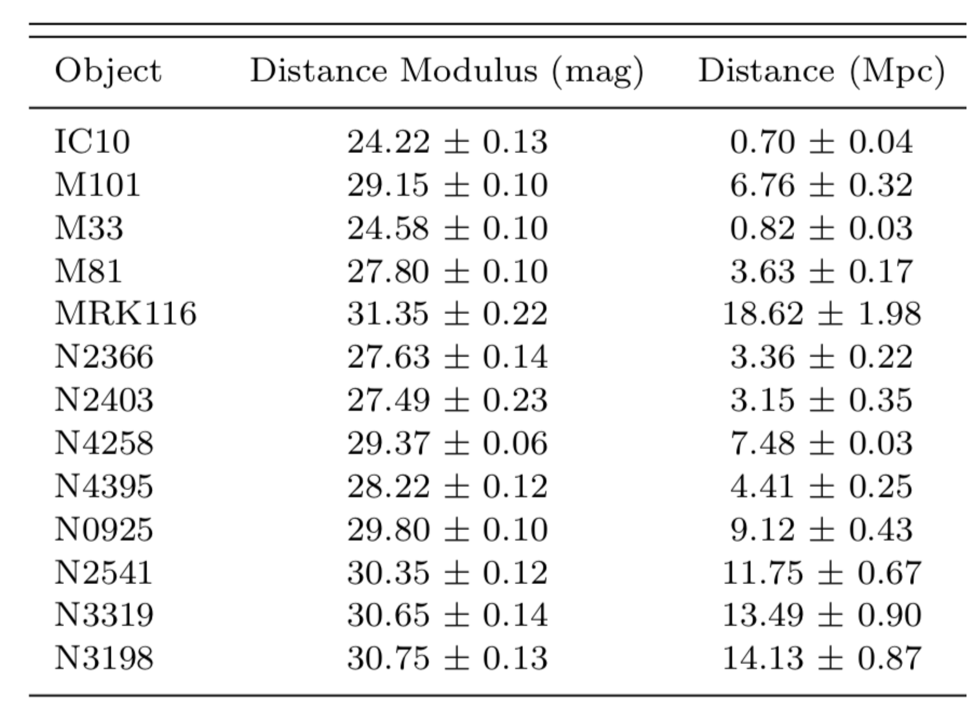

Object	Distance Modulus (mag)	Distance (Mpc)
IC10	24.22 ± 0.13	0.70 ± 0.04
M101	29.15 ± 0.10	6.76 ± 0.32
M33	24.58 ± 0.10	0.82 ± 0.03
M81	27.80 ± 0.10	3.63 ± 0.17
MRK116	31.35 ± 0.22	18.62 ± 1.98
N2366	27.63 ± 0.14	3.36 ± 0.22
N2403	27.49 ± 0.23	3.15 ± 0.35
N4258	29.37 ± 0.06	7.48 ± 0.03
N4395	28.22 ± 0.12	4.41 ± 0.25
N0925	29.80 ± 0.10	9.12 ± 0.43
N2541	30.35 ± 0.12	11.75 ± 0.67
N3319	30.65 ± 0.14	13.49 ± 0.90
N3198	30.75 ± 0.13	14.13 ± 0.87

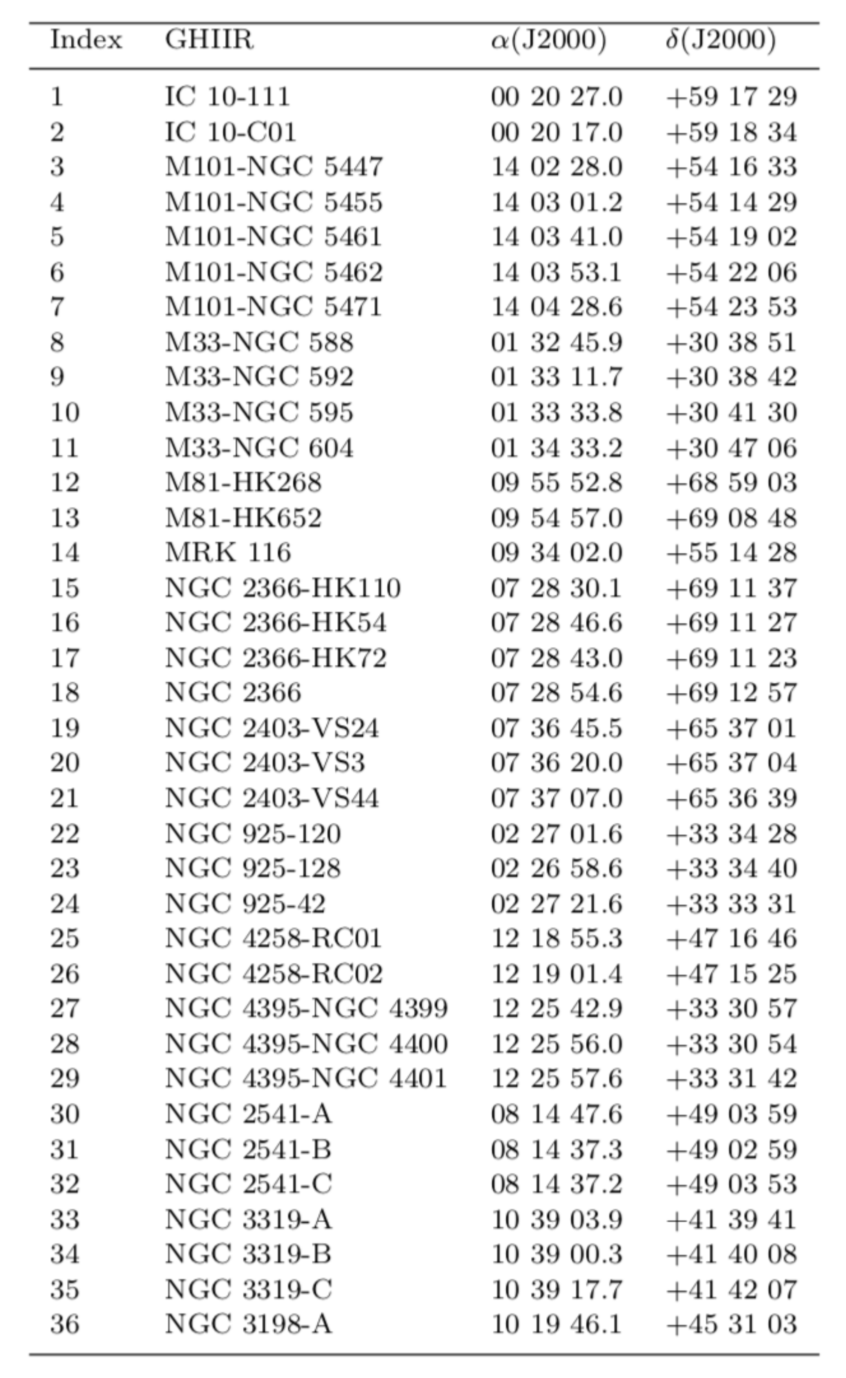

Index	GHIIR	α(J2000)	δ(J2000)
1	IC 10-111	00 20 27.0	+59 17 29
2	IC 10-C01	00 20 17.0	+59 18 34
3	M101-NGC 5447	14 02 28.0	+54 16 33
4	M101-NGC 5455	14 03 01.2	+54 14 29
5	M101-NGC 5461	14 03 41.0	+54 19 02
6	M101-NGC 5462	14 03 53.1	+54 22 06
7	M101-NGC 5471	14 04 28.6	+54 23 53
8	M33-NGC 588	01 32 45.9	+30 38 51
9	M33-NGC 592	01 33 11.7	+30 38 42
10	M33-NGC 595	01 33 33.8	+30 41 30
11	M33-NGC 604	01 34 33.2	+30 47 06
12	M81-HK268	09 55 52.8	+68 59 03
13	M81-HK652	09 54 57.0	+69 08 48
14	MRK 116	09 34 02.0	+55 14 28
15	NGC 2366-HK110	07 28 30.1	+69 11 37
16	NGC 2366-HK54	07 28 46.6	+69 11 27
17	NGC 2366-HK72	07 28 43.0	+69 11 23
18	NGC 2366	07 28 54.6	+69 12 57
19	NGC 2403-VS24	07 36 45.5	+65 37 01
20	NGC 2403-VS3	07 36 20.0	+65 37 04
21	NGC 2403-VS44	07 37 07.0	+65 36 39
22	NGC 925-120	02 27 01.6	+33 34 28
23	NGC 925-128	02 26 58.6	+33 34 40
24	NGC 925-42	02 27 21.6	+33 33 31
25	NGC 4258-RC01	12 18 55.3	+47 16 46
26	NGC 4258-RC02	12 19 01.4	+47 15 25
27	NGC 4395-NGC 4399	12 25 42.9	+33 30 57
28	NGC 4395-NGC 4400	12 25 56.0	+33 30 54
29	NGC 4395-NGC 4401	12 25 57.6	+33 31 42
30	NGC 2541-A	08 14 47.6	+49 03 59
31	NGC 2541-B	08 14 37.3	+49 02 59
32	NGC 2541-C	08 14 37.2	+49 03 53
33	NGC 3319-A	10 39 03.9	+41 39 41
34	NGC 3319-B	10 39 00.3	+41 40 08
35	NGC 3319-C	10 39 17.7	+41 42 07
36	NGC 3198-A	10 19 46.1	+45 31 03

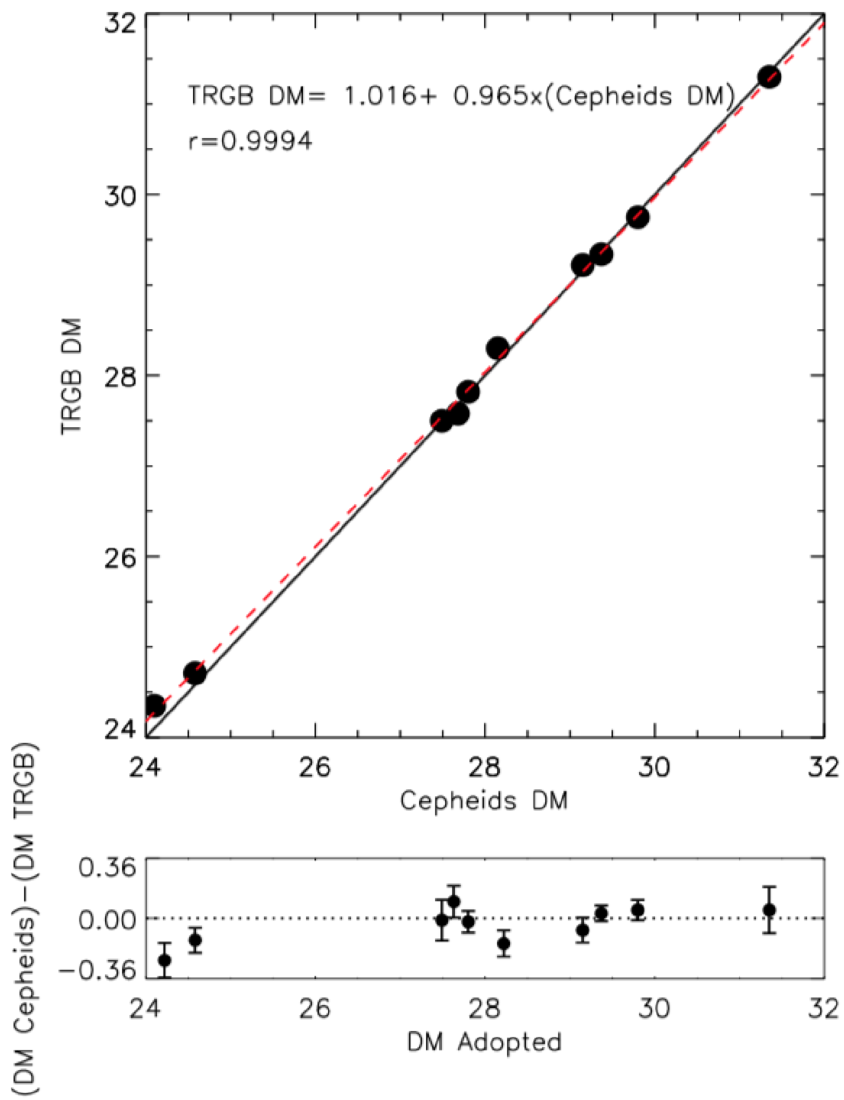

NEW GHIIR LOCAL CALIBRATION DATA

23 (in 9 galaxies) -> 36 (in 13 galaxies)

Arenas-Fernandez et al. 2018

same **Ho=74.6 (±2.9)** unless one uses evolutionary corrections in which case **Ho=71.0 (±2.8) only random errors !**

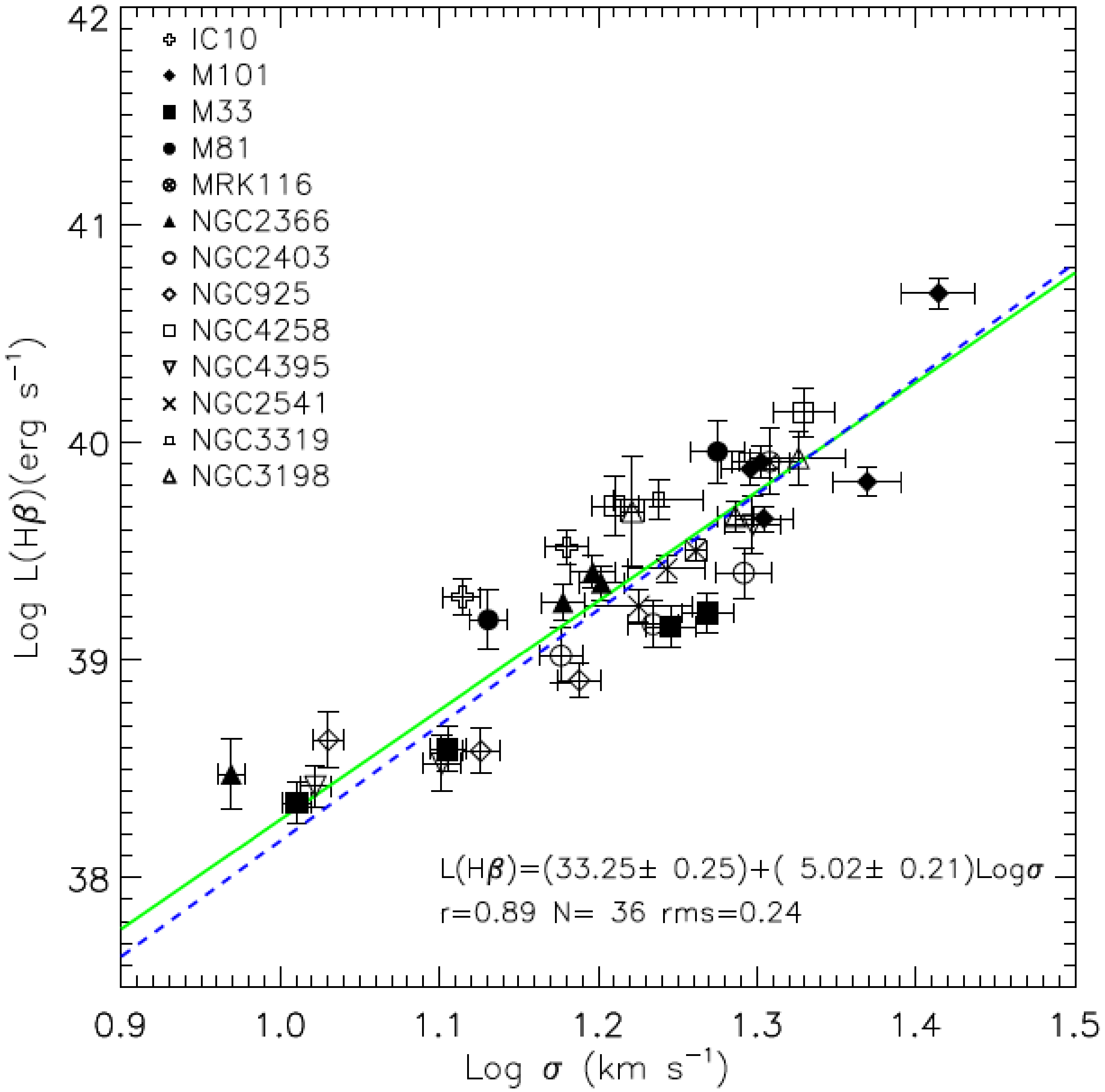

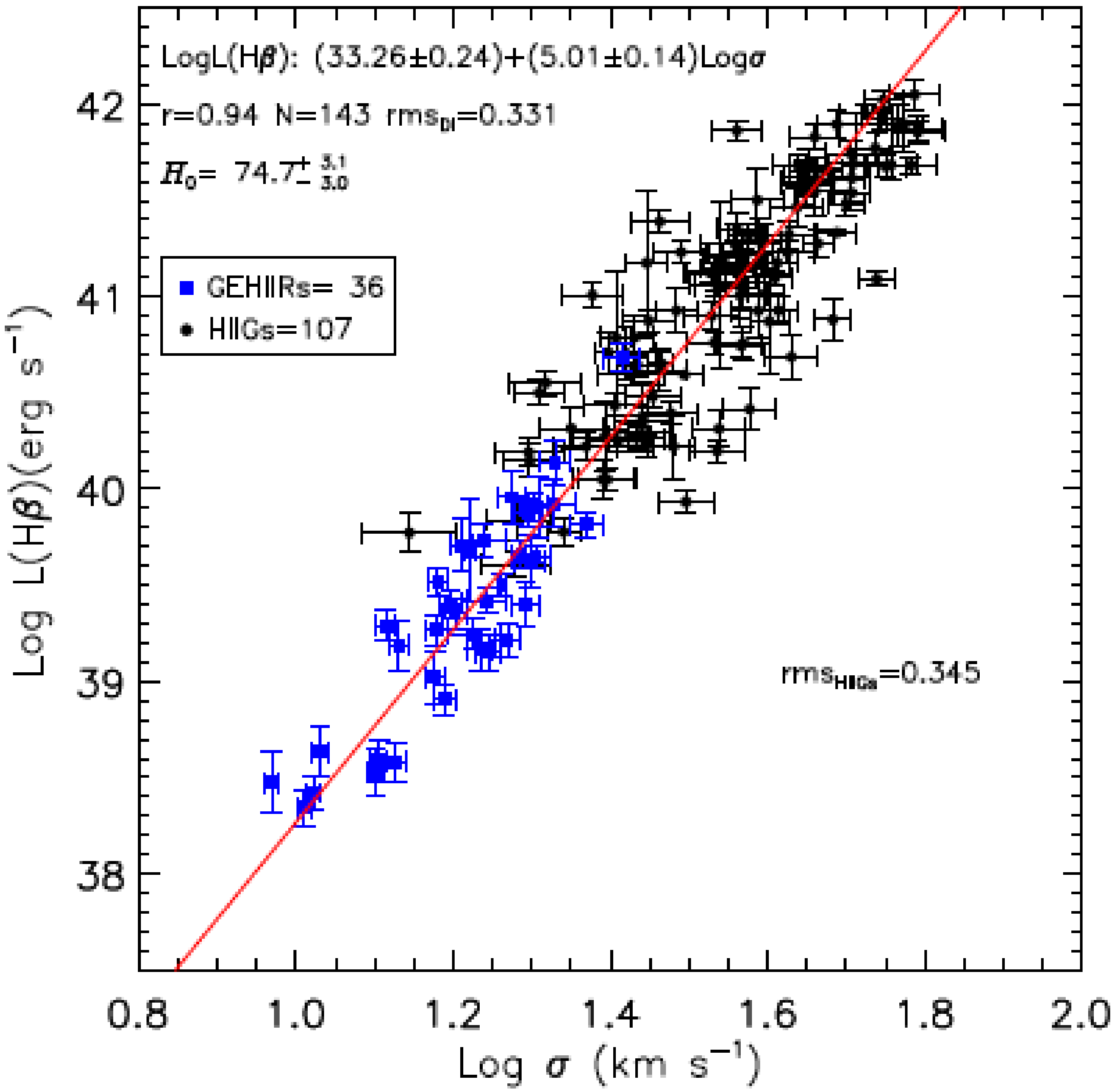

Age Correction

The ionising UV luminosity and thus emission-line luminosity drops within the first 5-7 Myr while continuum remains constant. This could introduce systematic effects, eg., if average GHIIR or HII ages are different or a function of z (note however that EW distributions are similar).

We use stellar population synthesis models SB99 models for a Kroupa IMF with Mup=120 M⊙ and Geneva tracks (Blue and Red Points correspond to two different metallicities).

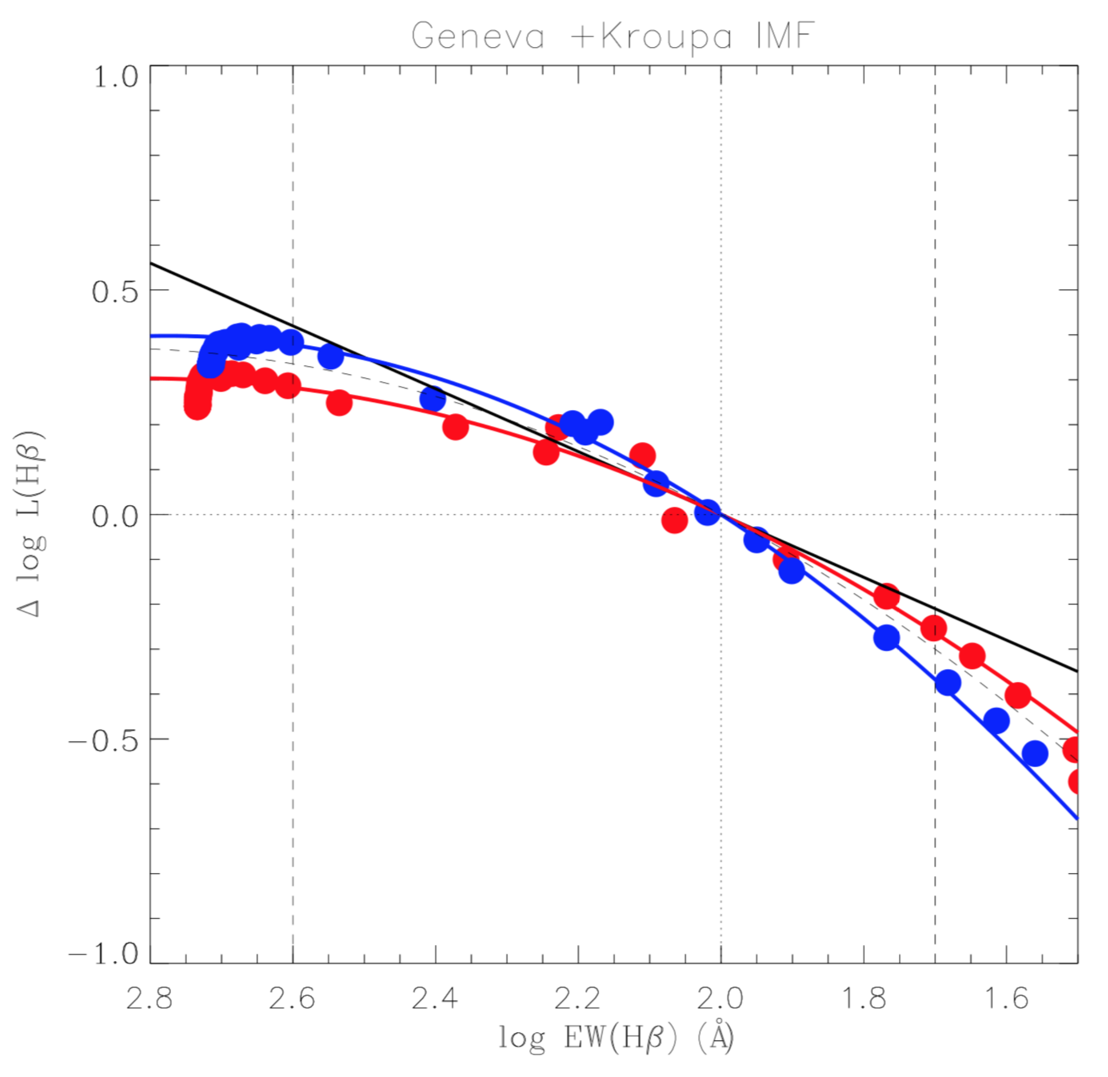

Finally, we correct Hβ luminosities to the value at an age corresponding to the median EW(Hβ) that for both GHIIR and HIIG it is 100Å, but many caveats exist, eg. SB99 does not include massive inter.binaries or M> 120Msolar stars, expected in SSC's -> INDICATIVE RESULTS

Systematics

Genuine systematic errors are difficult to estimate. To quantify at least part of the systematic error component we explored alternative parametrizations that can not be easily included in the error scheme.

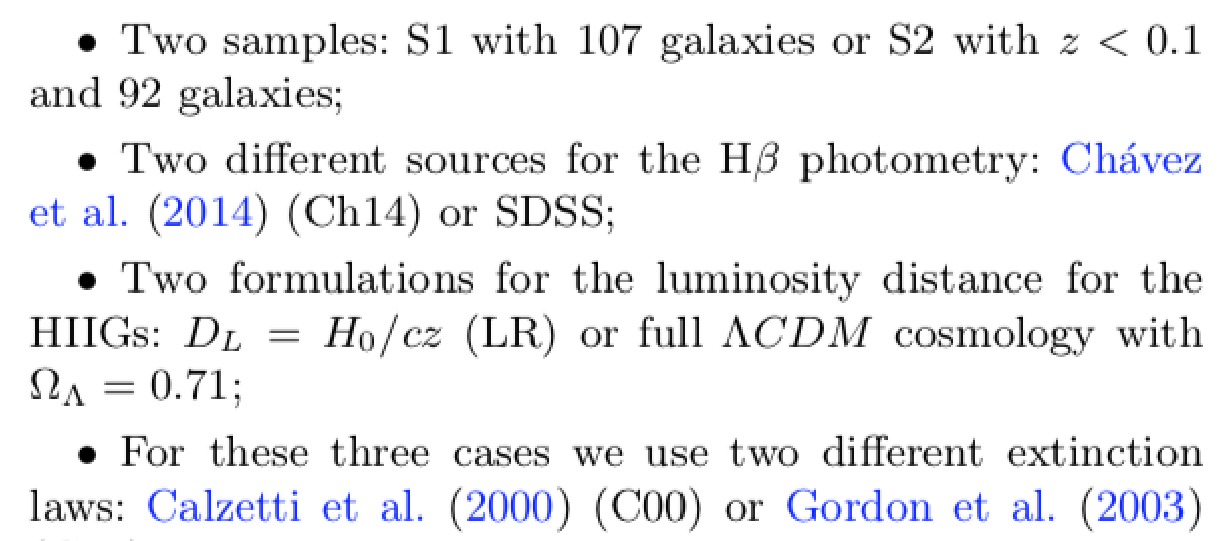

- Two samples: S1 with 107 galaxies or S2 with $z < 0.1$ and 92 galaxies;
- Two different sources for the Hβ photometry: Chávez et al. (2014) (Ch14) or SDSS;
- Two formulations for the luminosity distance for the HIIGs: $D_L = H_0/cz$ (LR) or full ΛCDM cosmology with $\Omega_\Lambda = 0.71$;
- For these three cases we use two different extinction laws: Calzetti et al. (2000) (C00) or Gordon et al. (2003)

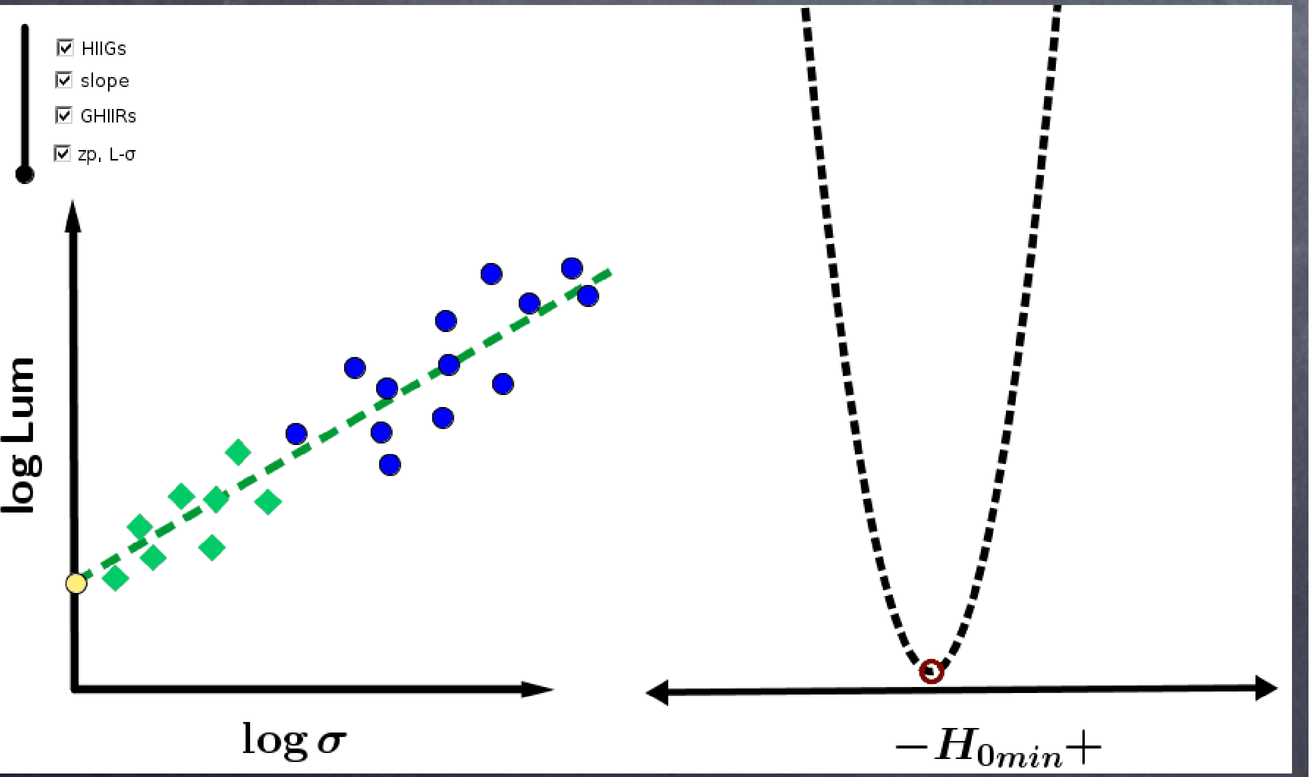

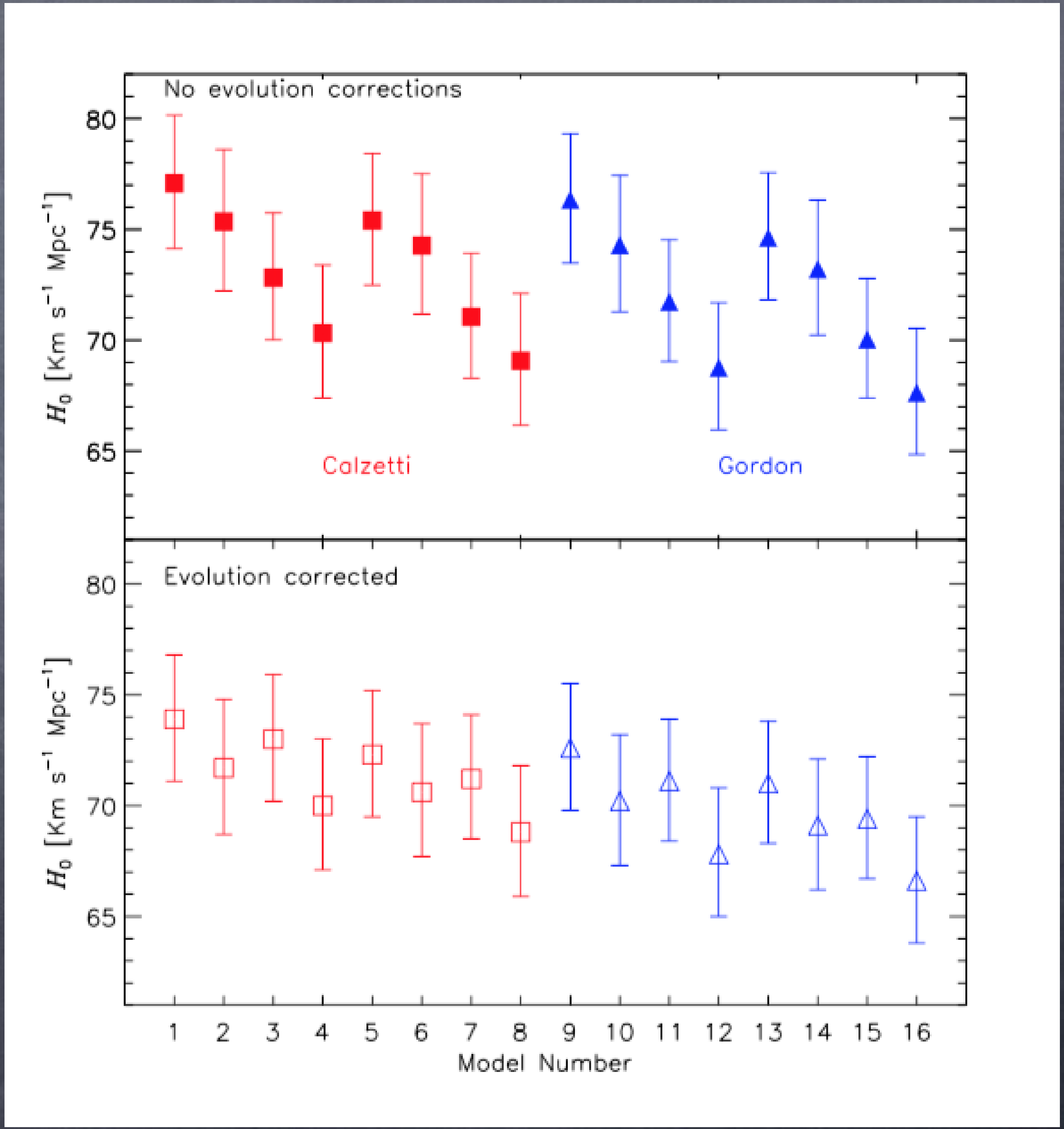

H_0 Tension

Cepheid-calibrated SNIa determinations:

1. Riess et al 2009: $H_0 = 74.2 \pm 3.6$ (random+systematic)
2. Riess et al 2012: $H_0 = 73.8 \pm 2.4$ (random+systematic)
3. Riess et al 2016: $H_0 = 73.2 \pm 1.7$ (random+systematic)
4. Riess et al 2022: **$H_0 = 73.0 \pm 1.04$** (random+systematic)

TRGB-calibrated SNIa determinations

1. Freedman et al 2021: **$H_0 = 69.8 \pm 0.6$ (rand) ± 1.6 (syst.)**

Cepheid-calibrated HII determinations

1. Chavez et al 2012: **$H_0 = 74.3 \pm 4.2$ (random+sys.)**

2. Fernandez-Arenas et al 2018: **$H_0 = 74.6 \pm 2.9$** (rand.) **± 2.5** (sys.) No Evol.
$H_0 = 71.0 \pm 2.8$ (rand.) **± 1.5** (sys.) Evol. Cor.

Planck+ΛCDM 2020: $H_0 = 67.4 \pm 0.5$ km/sec/Mpc

Planck+ΛCDM 2014: $H_0 = 67.2 \pm 1.2$ km/sec/Mpc
WMAP-9yr +ΛCDM 2013: $H_0 = 69.7 \pm 2.5$ km/sec/Mpc

Measuring H_0 - Final comments

(a) While the uncertainty in distance for a Giant HII region or HII galaxies is about 3 times larger than that of the SNIa there are more than one HII region per galaxy (typically 2-3),
(b) many nearby galaxies with Cepheids and HII regions
(c) 100 GHIIR in nearby galaxies with redshift independent distances
(d) Z<0.15 HIIG's are many hundreds

Next steps:

(1) add to the anchor sample ~50 GHIIR in 20 additional galaxies with Cepheid and/or TRGB distances making a total of ~90 GHIIR in 33 galaxies (in total 73 galaxies with 130 GHIIR).
(2) We are also increasing the sample of nearby (0.02 <z< 0.16) HIIG
(3) we are reviewing all the corrections applied to the data, particularly the evolution and extinction corrections
(4) Aim to reduce significantly random and systematic errors.

2nd Application: High-z HII Cosmological Constraints

HIGH-Z SAMPLE SELECTION

For MOSFIRE-KECK and KMOS-VLT observations

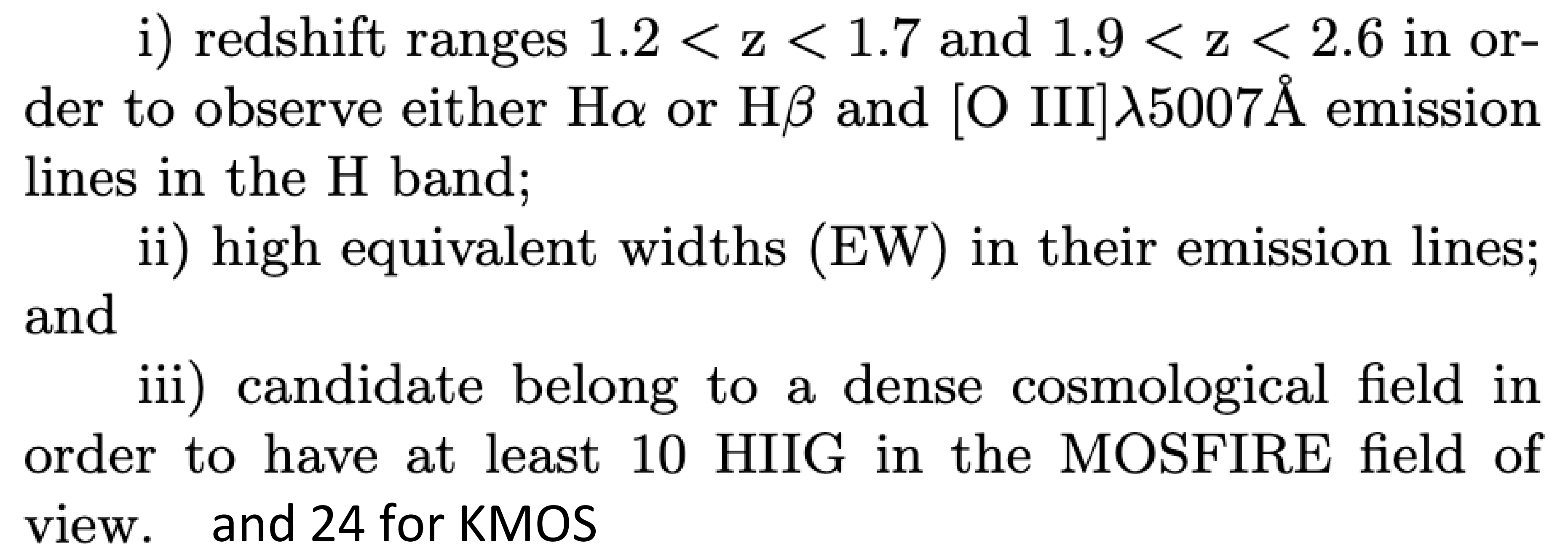

i) redshift ranges $1.2 < z < 1.7$ and $1.9 < z < 2.6$ in order to observe either Hα or Hβ and [O III]λ5007Å emission lines in the H band;

ii) high equivalent widths (EW) in their emission lines; and

iii) candidate belong to a dense cosmological field in order to have at least 10 HIIG in the MOSFIRE field of view. and 24 for KMOS

3 cosmological fields: the Ultra Deep Survey (UDS; Lawrence et al. 2007; Cirasuolo et al. 2007), GOODS-South Deep (GSD; Giavalisco et al. 2004) and the Cosmic Evolution Survey (COSMOS; Scoville et al. 2007; Koekemoer et al. 2007)

Common HIIG's observed to check consistency

2nd Application: High-z HII Cosmological Constraints

Chavez, Plionis, Basilakos et al. 2016
Gonzalez-Moran et al. 2019, 2021
Tsiapi et al 2021, Mehrabi et al 2021

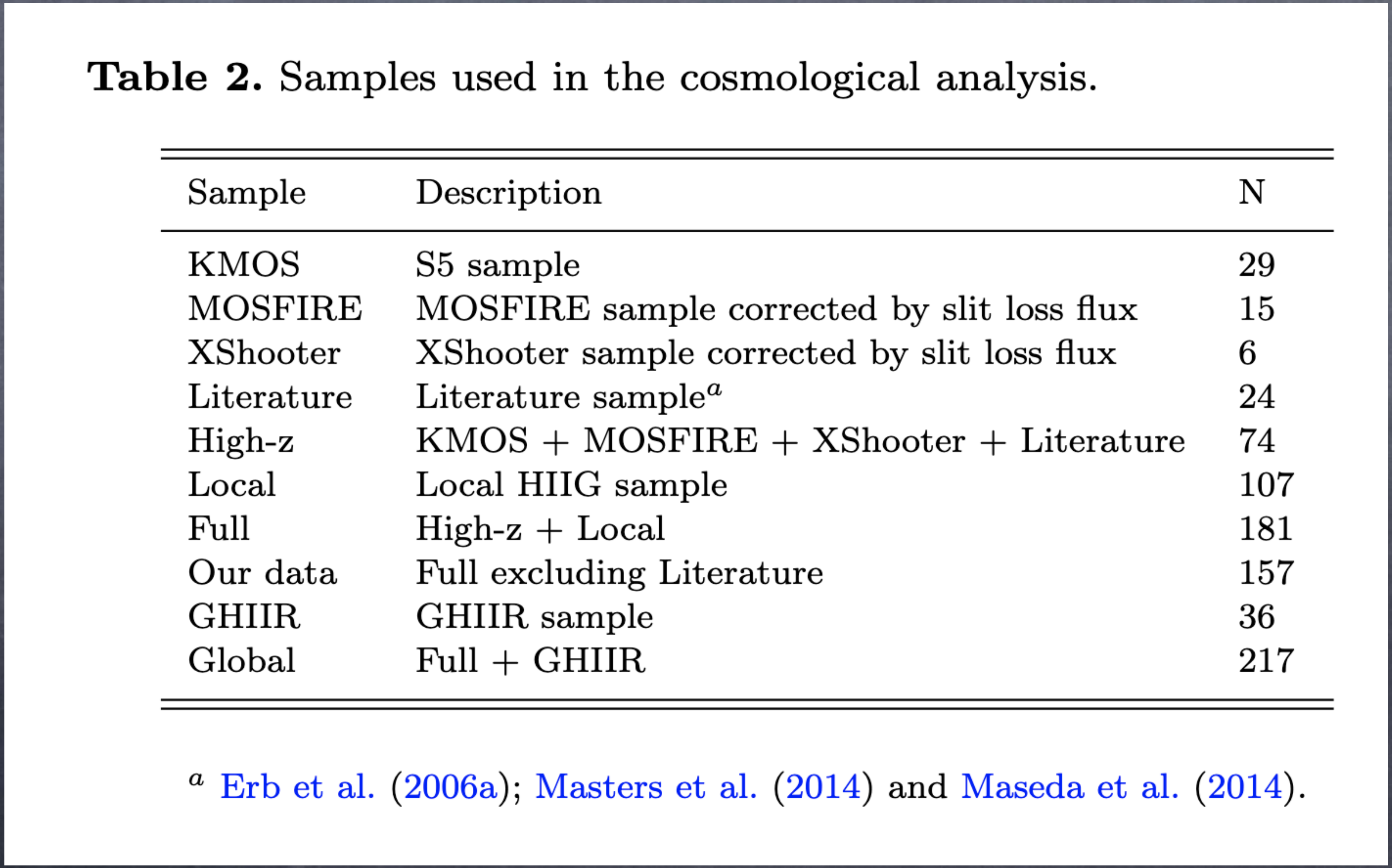

Table 2. Samples used in the cosmological analysis.

Sample	Description	N
KMOS	S5 sample	29
MOSFIRE	MOSFIRE sample corrected by slit loss flux	15
XShooter	XShooter sample corrected by slit loss flux	6
Literature	Literature sample[a]	24
High-z	KMOS + MOSFIRE + XShooter + Literature	74
Local	Local HIIG sample	107
Full	High-z + Local	181
Our data	Full excluding Literature	157
GHIIR	GHIIR sample	36
Global	Full + GHIIR	217

[a] Erb et al. (2006a); Masters et al. (2014) and Maseda et al. (2014).

Stamp Images of high-z HII Galaxies

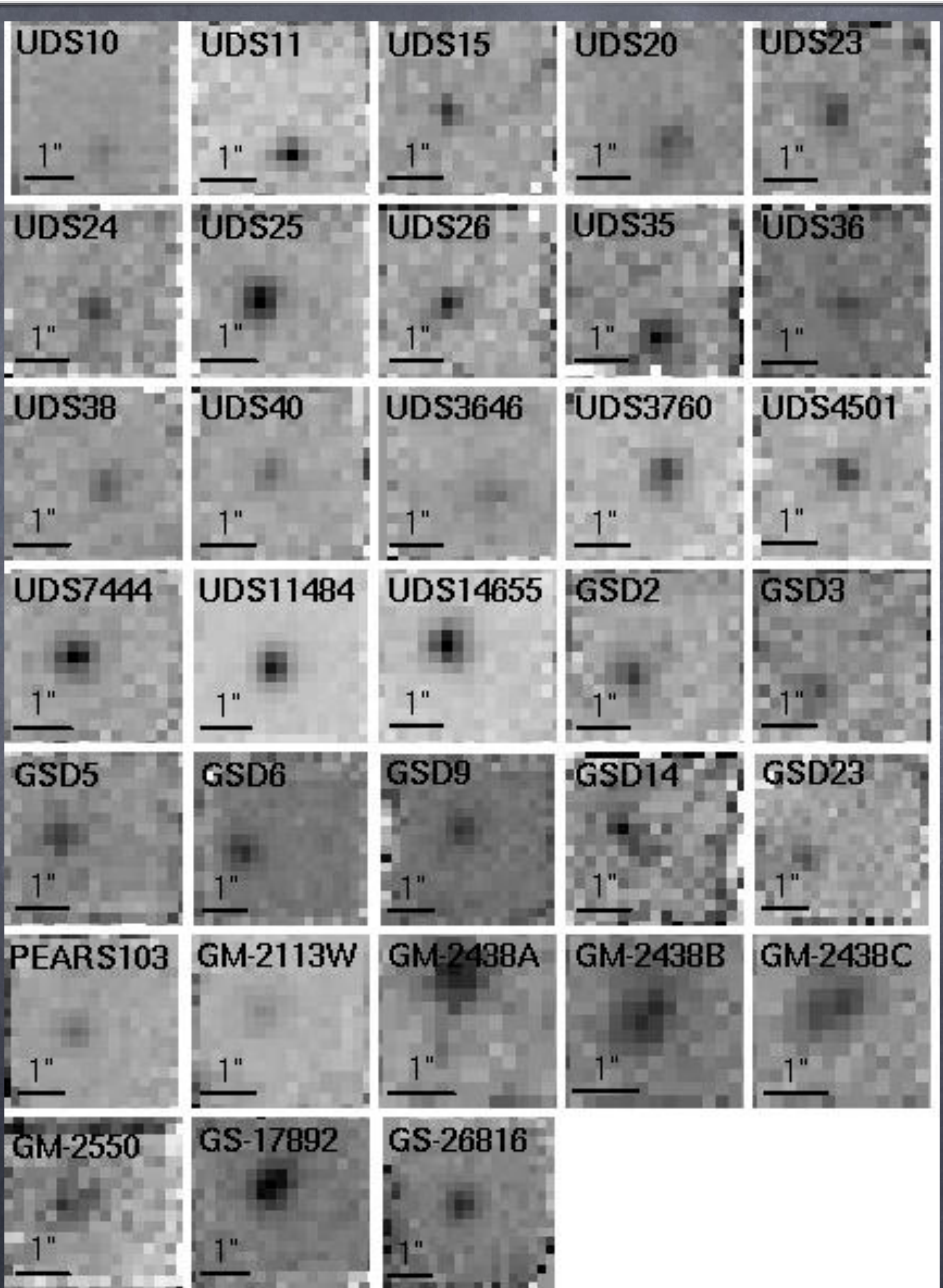

2nd Application: High-z HII Cosmological Constraints

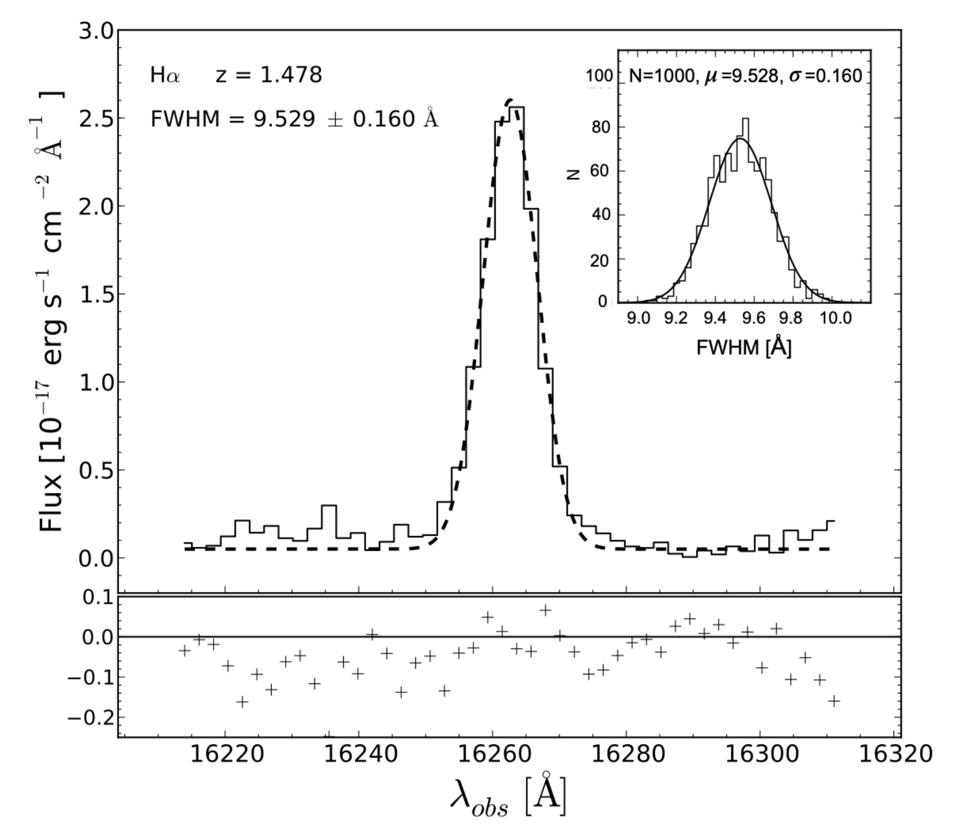

Gonzalez-Moran et al. 2021

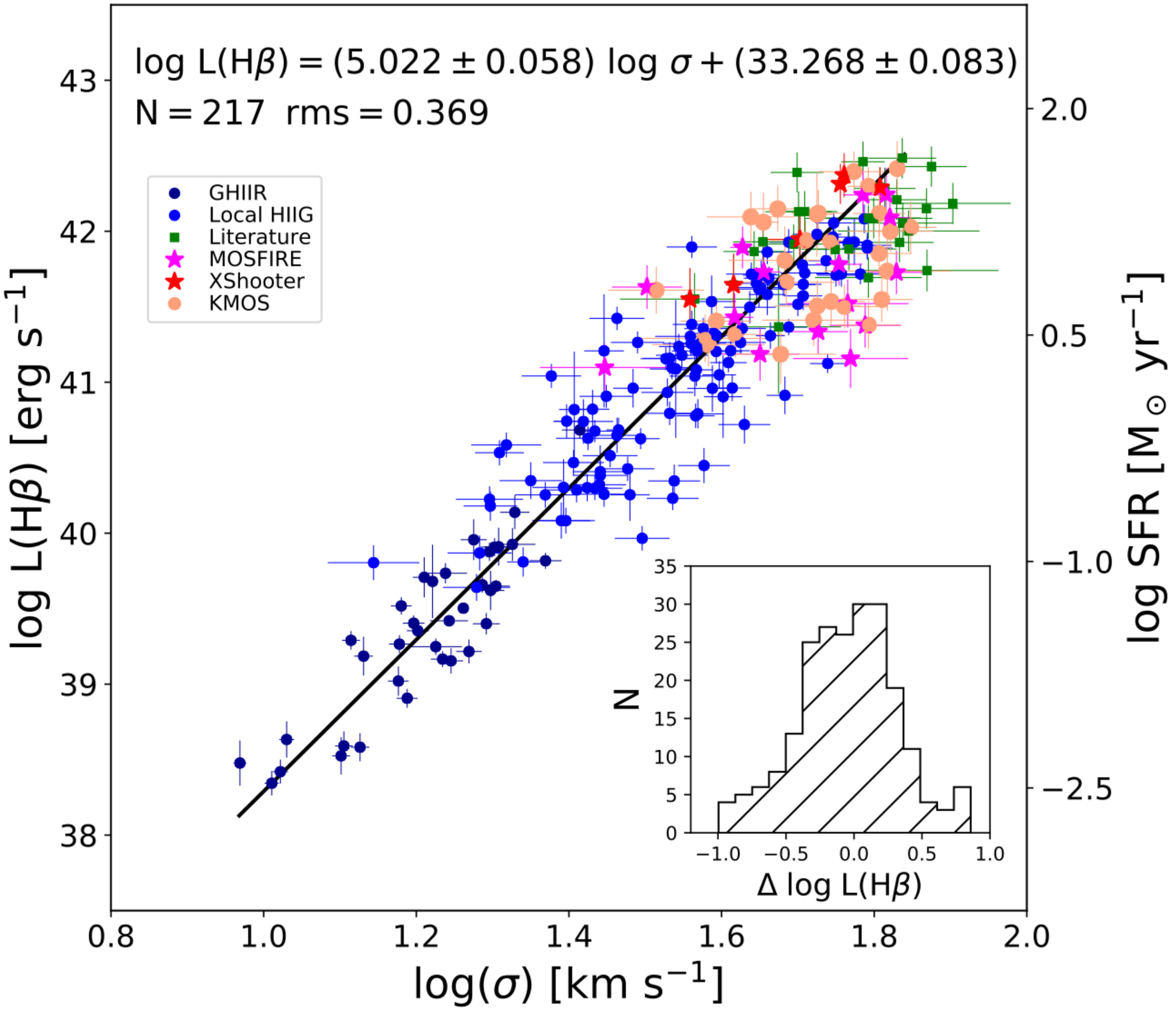

2nd Application: High-z HII Cosmological Constraints

The current HII Hubble diagram

Gonzalez-Moran et al. 2021

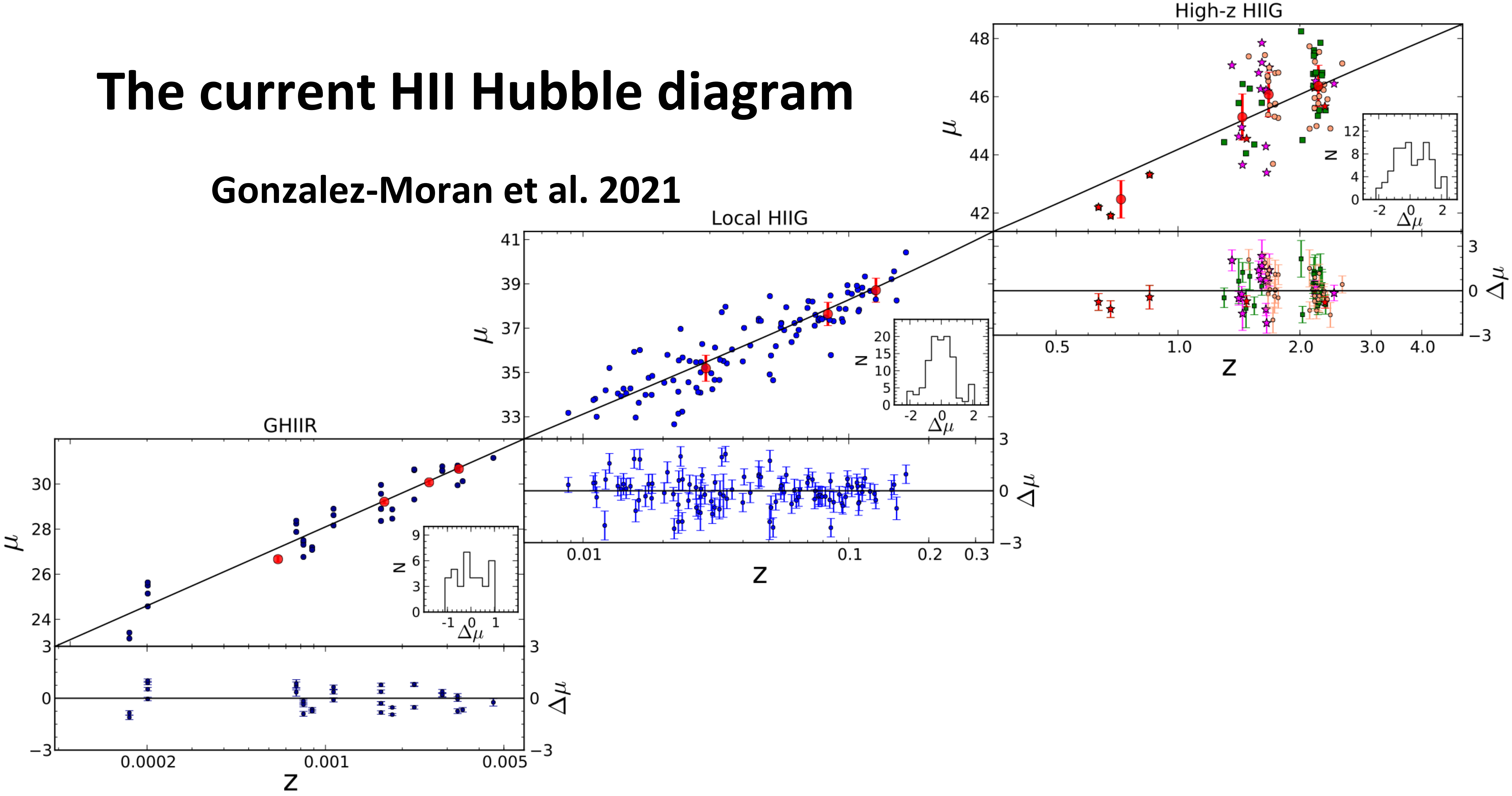

2nd Application: High-z HII Cosmological Constraints

The current HII & SNia Hubble diagram

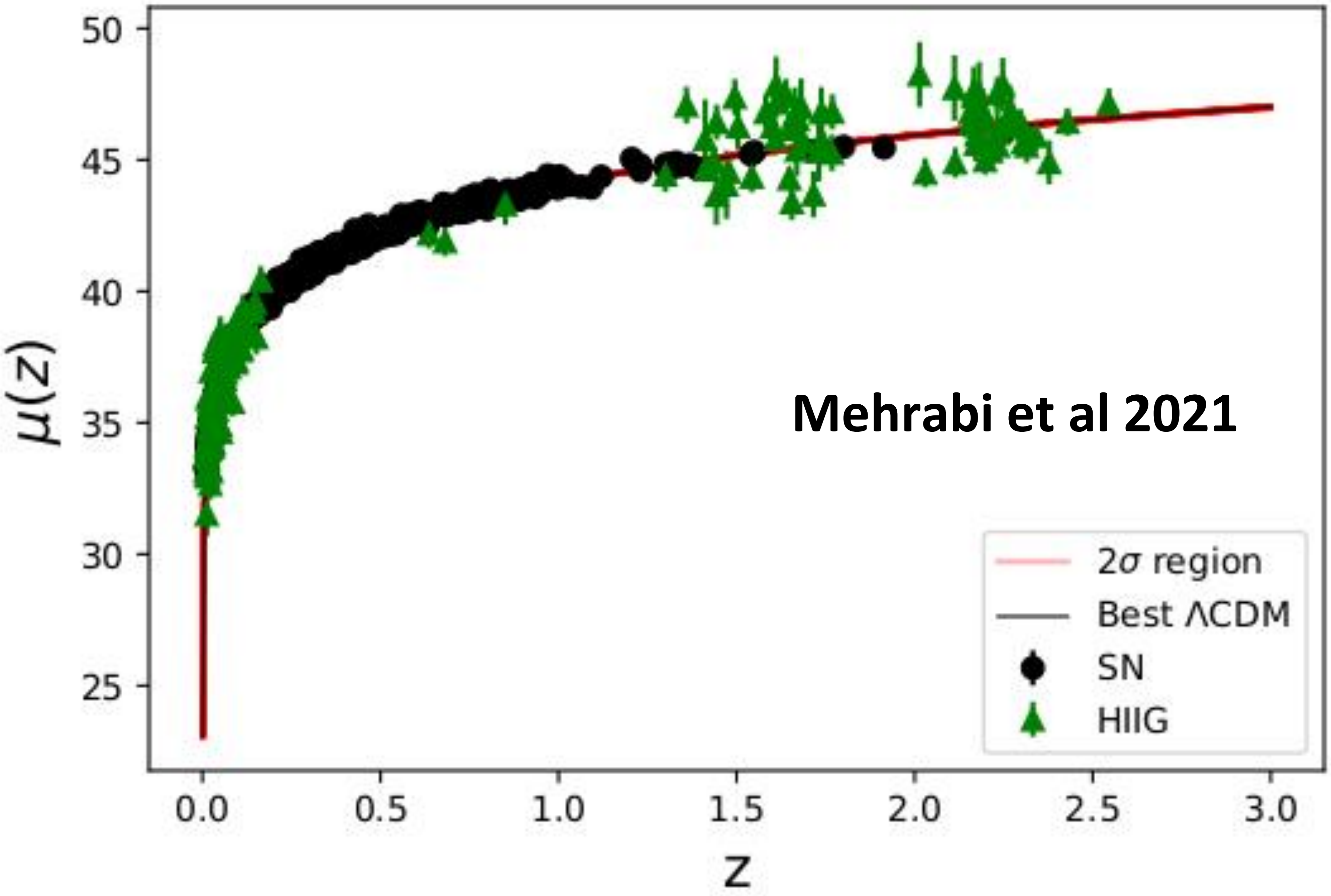

Mehrabi et al 2021

2nd Application: High-z HII Cosmological Constraints

Gonzalez-Moran et al. 2021

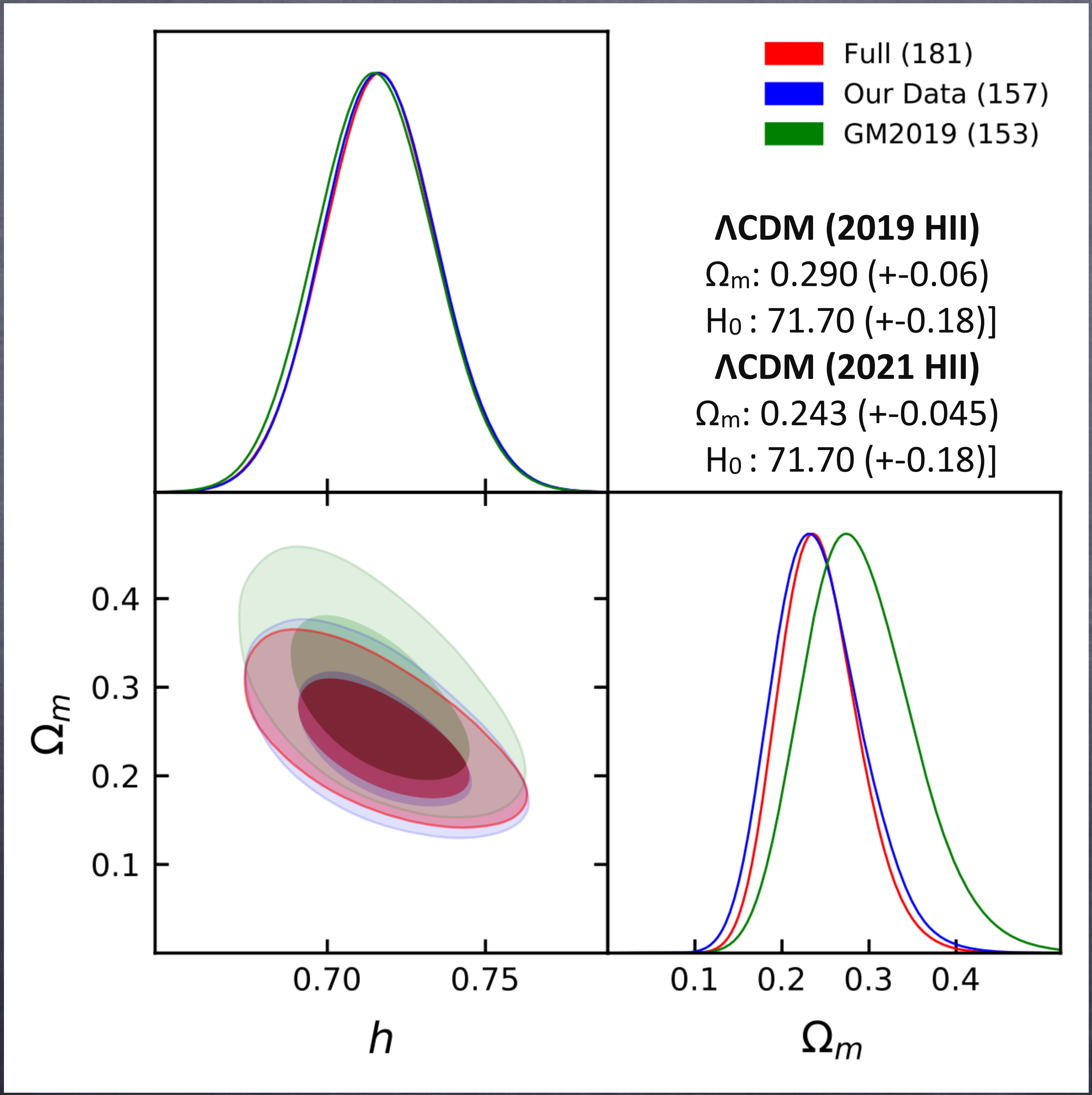

ΛCDM (2019 HII)

Ω_m: 0.290 (+-0.06)

H_0 : 71.70 (+-0.18)]

ΛCDM (2021 HII)

Ω_m: 0.243 (+-0.045)

H_0 : 71.70 (+-0.18)]

2nd Application: High-z HII Cosmological Constraints

Gonzalez-Moran et al. 2021

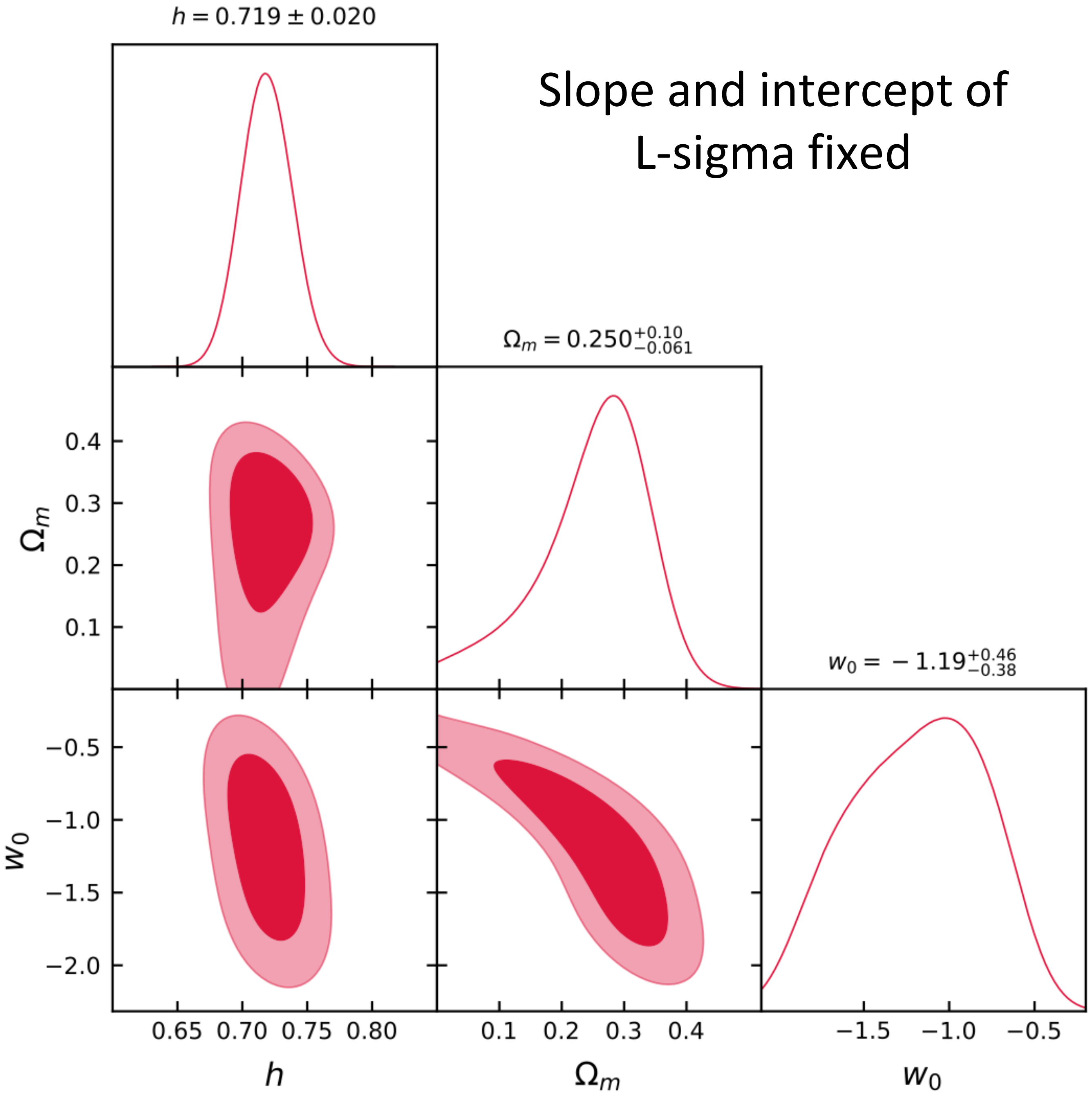

Slope and intercept of L-sigma fixed

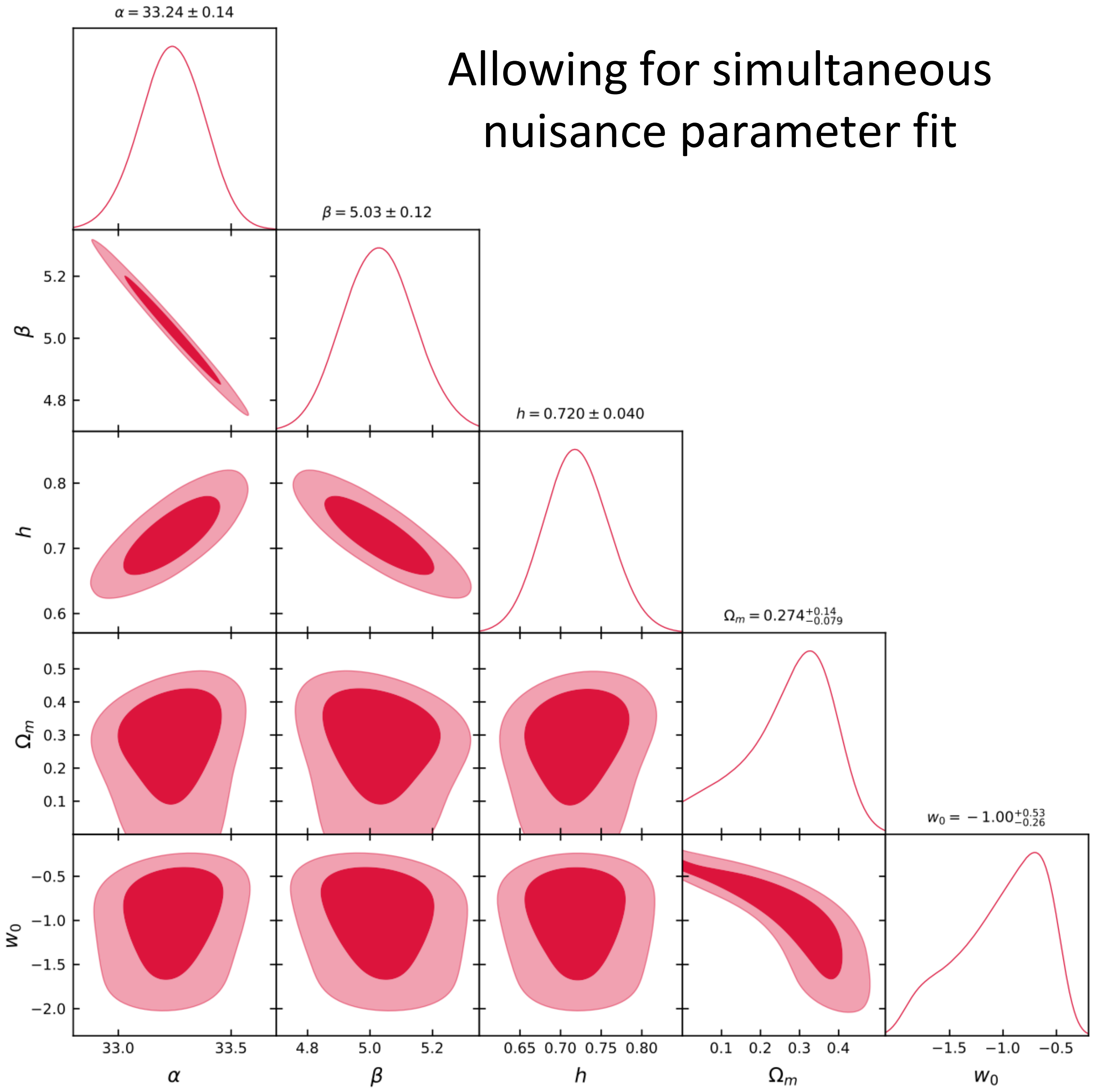

Allowing for simultaneous nuisance parameter fit

<u>2nd Application</u>: High-z HII Cosmological Constraints

Comparing the Performance of SNIa (Pantheon) and HII's

Using a Joint analysis with BAO (6d Field, WiggleZ DES, SDSS-III) & CMB (shift parameter+acoustic scale) we find:

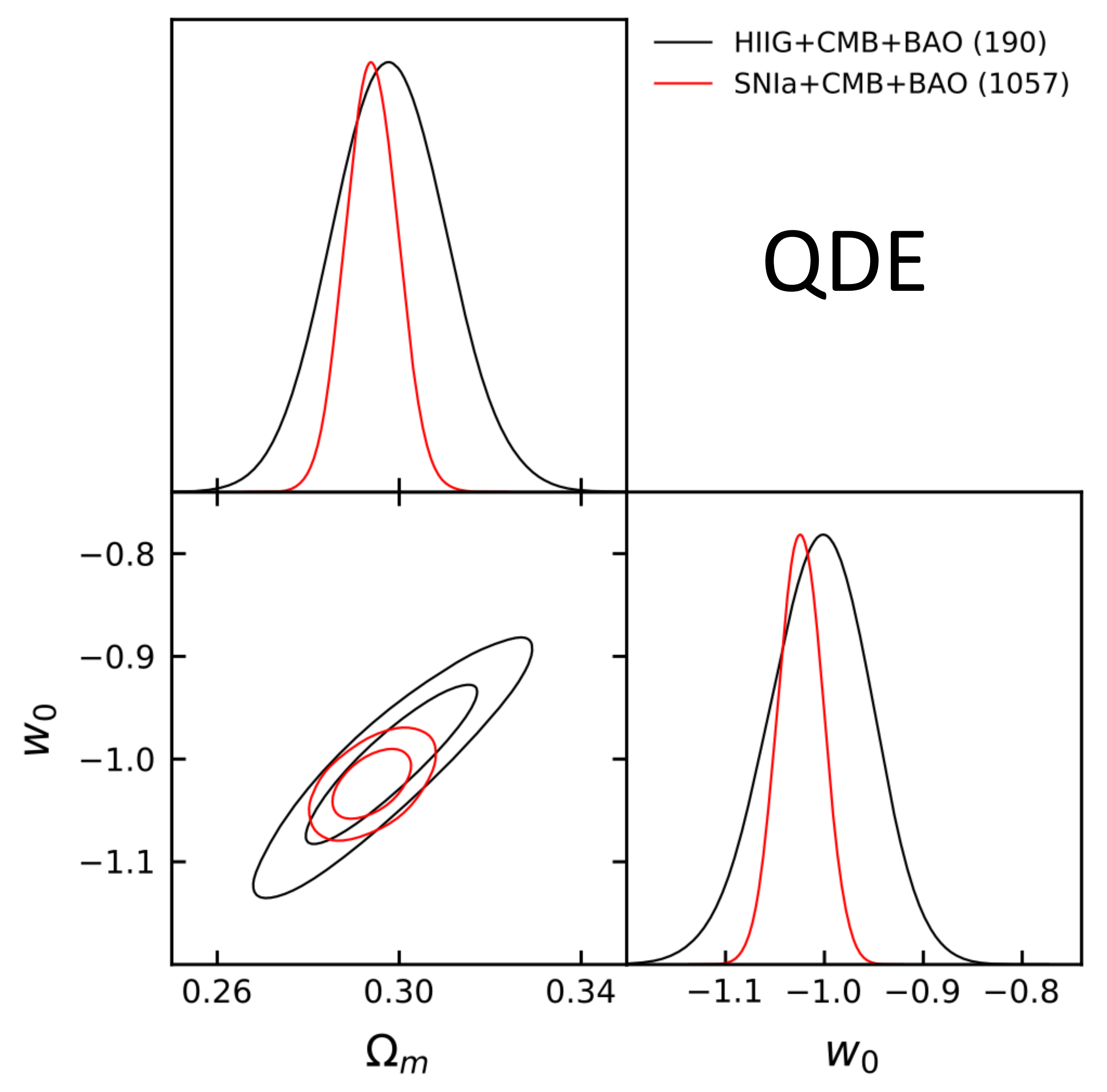

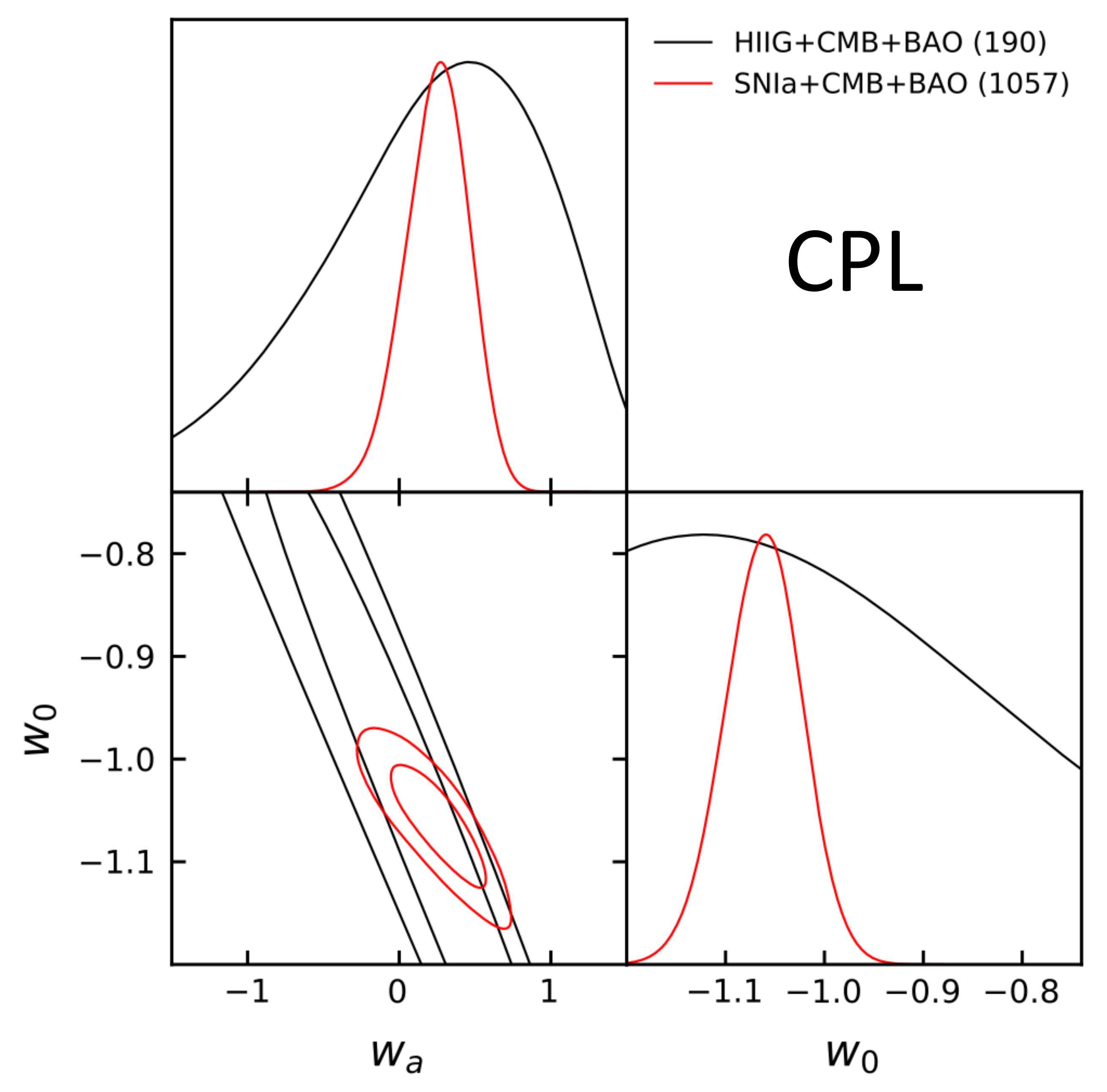

2nd Application: High-z HII Cosmological Constraints

Chavez, Plionis, Basilakos et al. 2016

We have performed extensive simulations to determine necessary numbers of high-z HII galaxies to be observed in order to increase the Figure of Merit by a given amount.

Until recently there was no instrument in a 10m class telescope capable of obtaining multiple spectra of moderate dispersion (R>4000) in the near IR ~ 2 microns.

Currently MOSFIRE at KECK & KMOS at VLT & EMIR at GTC (2018)

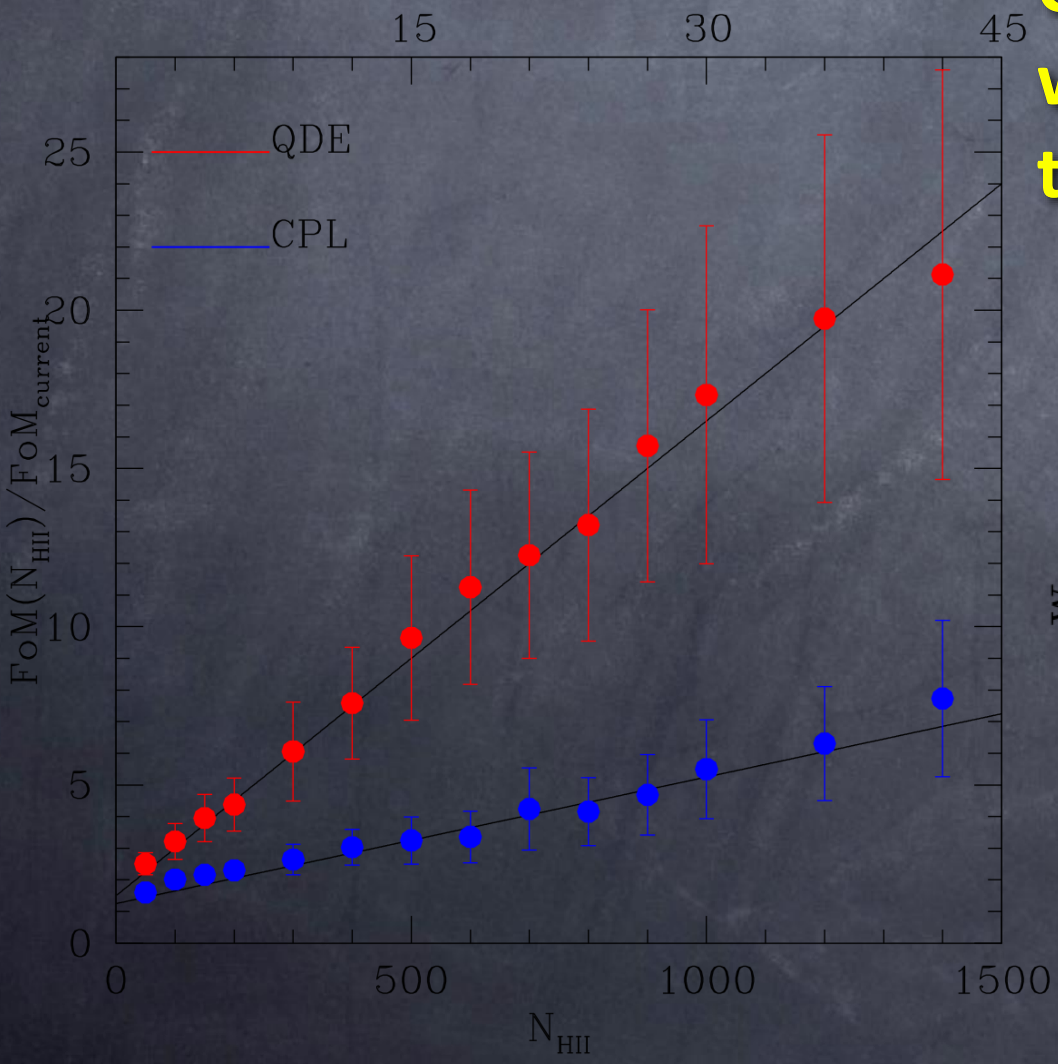

Comparing the current constraints (red contours) with the expected for 500 high-z HII galaxies, for the QDE & CPL DE EoS.

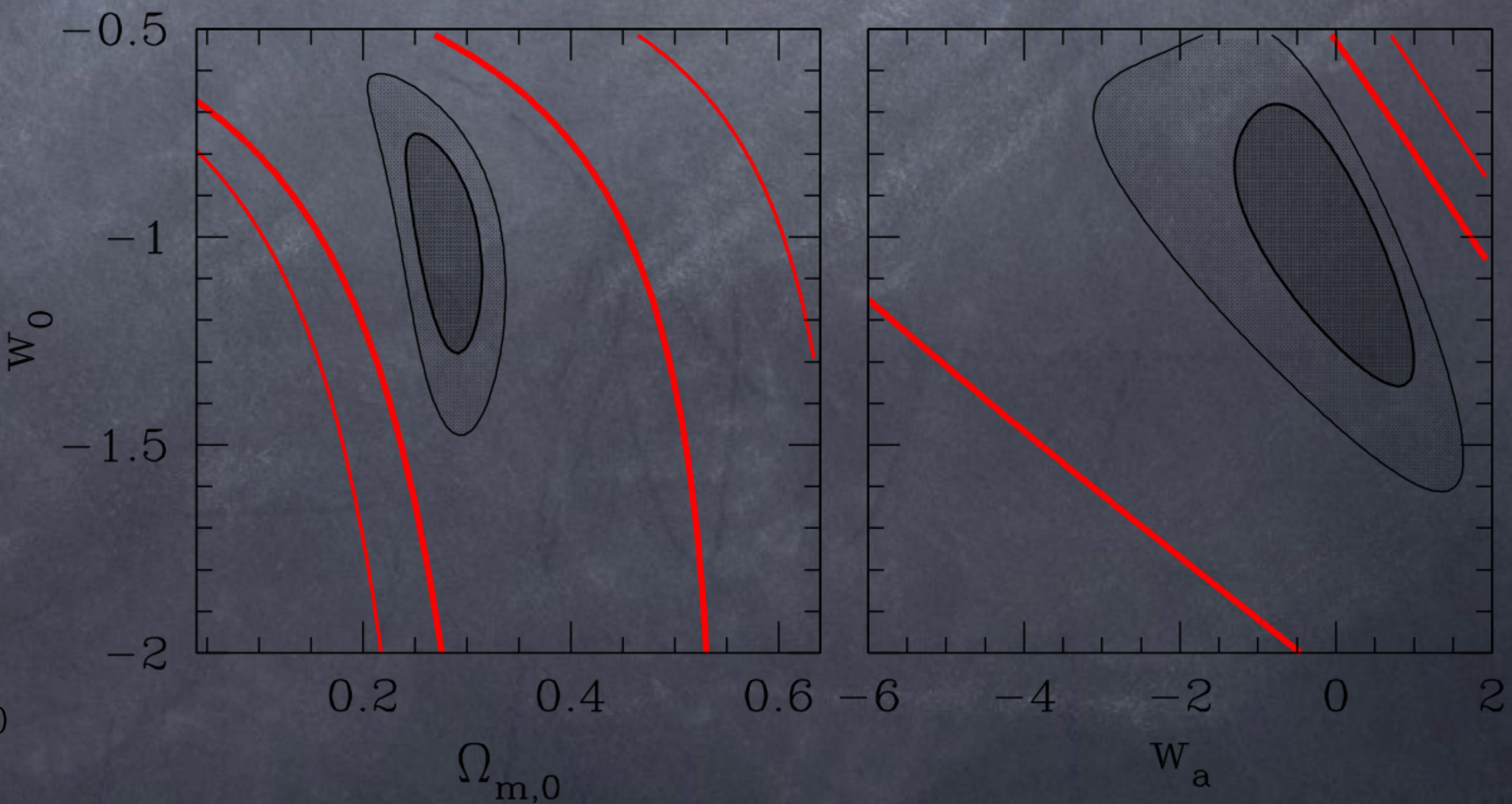

Concluding Remarks

- **High redshift ($2<z<3.5$) tracers are very useful for the Hubble expansion Probe in order to obtain better constraints** to the Cosmological Parameters space and distinguish among Dark Energy models.
- **We have shown the viability of using H II galaxies as an alternative H(z) tracer: (a)** Ho tension persists, we find **$H_0=74.6 \pm 2.9 \pm 2.4$ km/s/Mpc** in excellent agreement with SNIa, while using a evolution model **$H_0=71 \pm 2.8 \pm 1.5$ km/s/Mpc**. **Age corrections are indicative and should be scrutinised. (b) Our current high-z HII galaxy sample (74 galaxies only)** gives consistent but significantly weaker **Ω_m-w and w_0-w_a** constraints than those of SNIa.
- **Monte-Carlo simulations show that future HII observations will provide stringent DE EoS parameter constraints**.
- **We cannot compete with SNIa but rather develop the use of an alternative high-z Hubble-expansion tracer, that goes deeper, to check consistency of results.**